(4)

TR 89001
JANUARY

Final Report

SCALEABLE PROCESS FOR CVD OF LARGE-AREA HETEROEPITAXIAL β-SiC ON TiC$_x$ USING GASES WITH 1:1 SILICON TO CARBON STOICHIOMETRY

Submitted by:

Diamond Materials Institute, Inc.
2820 East College Avenue
State College, PA

Contract #N00014-88-C-0549

Contract Period:
July 1, 1988 to December 31, 1988

January 30, 1989

Research Supported by
Strategic Defense Initiative/Innovative
Science and Technology
Managed by
Office of Naval Research

Diamond Materials Institute

SECURITY CLASSIFICATION OF THIS PAGE

REPORT DOCUMENTATION PAGE

1a REPORT SECURITY CLASSIFICATION: Unclassified	1b RESTRICTIVE MARKINGS
2a SECURITY CLASSIFICATION AUTHORITY	3 DISTRIBUTION / AVAILABILITY OF REPORT: Approved for public release; distribution unlimited
2b DECLASSIFICATION / DOWNGRADING SCHEDULE	
4 PERFORMING ORGANIZATION REPORT NUMBER(S)	5 MONITORING ORGANIZATION REPORT NUMBER(S)
6a NAME OF PERFORMING ORGANIZATION: Diamond Materials Institute, Inc. / 6b OFFICE SYMBOL (If applicable)	7a. NAME OF MONITORING ORGANIZATION: Office of Naval Research
6c ADDRESS (City, State, and ZIP Code): 2820 East College Avenue, State College, PA 16801	7b. ADDRESS (City, State, and ZIP Code): Code 1114, Arlington, VA 22217-5000
8a. NAME OF FUNDING / SPONSORING ORGANIZATION: SDIO/IST / 8b. OFFICE SYMBOL (If applicable)	9. PROCUREMENT INSTRUMENT IDENTIFICATION NUMBER
8c. ADDRESS (City, State, and ZIP Code): The Pentagon, Washington, DC 20301-7100	10 SOURCE OF FUNDING NUMBERS: PROGRAM ELEMENT NO 63220C; PROJECT NO. SBIR; TASK NO. S405010srr; WORK UNIT ACCESSION NO 01

11 TITLE (Include Security Classification)
Scaleable Process for CVD of Large-Area Heteroepitaxial Beta-SiC on TiC Using Gases with 1:1 Si:C Stoichiometry

12 PERSONAL AUTHOR(S)
Koba, Richard; Kupp, Donald, and Phelps, Andrew

13a TYPE OF REPORT	13b. TIME COVERED	14 DATE OF REPORT (Year, Month, Day)	15 PAGE COUNT
Final Report	FROM 88/7/1 TO 88/12/30	1989, January 30	64

16 SUPPLEMENTARY NOTATION

17 COSATI CODES			18 SUBJECT TERMS (Continue on reverse if necessary and identify by block number)
FIELD	GROUP	SUB-GROUP	Heteroepitaxy, ~~β-SiC~~, TiC, stoichiometry, lattice, thermal expansion, Beta

19 ABSTRACT (Continue on reverse if necessary and identify by block number)

Diamond Materials Institute, Inc. (DMI) has demonstrated that single phase β-SiC films can be reliably deposited on TiC substrates using novel source gases with a 1:1 Si:C stoichiometry. In particular, DMI has demonstrated the growth of β-SiC from methylsilane + ethylene + hydrogen mixtures and from methyl trichlorosilane + hydrogen mixtures. In addition, DMI has demonstrated heteroepitaxial growth of monocrystalline β-SiC from mixtures of methyl trichlorosilane + hydrogen. Heteroepitaxial growth of β-SiC was demonstrated on a monocrystalline substrate of composition 95 mole % TiC + 5 mole % VC. The presence of 5% VC in TiC did not adversely affect the heteroepitaxial growth of β-SiC. During this program, DMI solved a number of practical problems

20 DISTRIBUTION / AVAILABILITY OF ABSTRACT	21. ABSTRACT SECURITY CLASSIFICATION
☒ UNCLASSIFIED/UNLIMITED ☐ SAME AS RPT ☐ DTIC USERS	Unclassified
22a NAME OF RESPONSIBLE INDIVIDUAL	22b TELEPHONE (Include Area Code) / 22c. OFFICE SYMBOL

DD FORM 1473, 84 MAR — 83 APR edition may be used until exhausted. All other editions are obsolete.

SECURITY CLASSIFICATION OF THIS PAGE

involved in the chemical vapor deposition of β-SiC at temperatures between 1250°C and 1400°C using an upward vertical flow reactor. DMI also discovered procedures necessary to ensure heteroepitaxial growth of β-SiC on (Ti,V)C substrates. In particular, DMI discovered a procedure to saturate (or nearly saturate) a TiC_x surface with bonded carbon immediately before the start of β-SiC deposition. TiC_x was found to be highly chemically reactive at 1400°C. During carburization, TiC_x can be etched by H_2 (or H°). During β-SiC deposition from methyl trichlorosilane, TiC_x can be etched by H_2, H° and/or HCl. DMI's success was based upon control of TiC_x etching during carburization and during β-SiC growth. DMI is now poised for an aggressive Phase II program to perform *in-situ* doping of β-SiC and create high-performance β-SiC semiconductor devices such as IMPATT diodes.

Final Report:

"Scaleable Process for CVD of Large-Area Heteroepitaxial β-SiC on TiC_x Using Gases with 1:1 Silicon to Carbon Stoichiometry"

Submitted by:

Diamond Materials Institute, Inc.
2820 East College Avenue
State College, PA 16801

Contract #N00014-88-C-0549

Contract Period:
July 1, 1988 to December 31, 1988

Report submitted:
January 30, 1989

Research Supported by Strategic Defense Initiative/Innovative Science and Technology and Managed by the Office of Naval Research.

1. MOTIVATION FOR THE RESEARCH

1.1 The Tremendous Promise of ß-SiC for Semiconductor Devices

ß-SiC holds the promise of being the most commercially important semiconductor since silicon. ß-SiC has many properties that are superior to silicon and GaAs. Two different figures of merit rate ß-SiC superior to silicon, GaAs, and InP semiconductors [1]. Table 1 lists various properties of semiconductor along with Key's Figure of Merit, which rates the theoretical performance of densely integrated circuits fabricated in the semiconductor. ß-SiC rates 5.8 times better than silicon according to Key's Figure of Merit. Table 2 lists other physical properties of semiconductors along with Johnson's Figure of Merit. Johnson's Figure of Merit rates the ability of the semiconductor to be used for microwave and millimeter wave power amplifiers and oscillators. As shown in Table 2, ß-SiC is 1137.8 times more suitable for high-frequency devices than silicon. Mehdi, Haddad and Mains [2] recently published a theoretical study of the potential of ß-SiC for double-drift IMPATT diodes. They concluded that ß-SiC IMPATTs could operate at much higher power (in pulsed mode and cw mode) than comparable Si or GaAs devices.

Another reason why ß-SiC may someday surpass GaAs as the second most commonly used semiconductor is that the chemical properties of ß-SiC are similar to the chemical properties of silicon. It should be straightforward for chip manufacturers to directly substitute ß-SiC for Si in integrated circuit fabrication lines. ß-SiC is similar to Si in that ß-SiC:

- has a shallow donor dopant, viz., nitrogen. Nitrogen can be incorporated controllably during epitaxial growth, or by ion implantation [3];
- has a shallow acceptor dopant, viz., aluminum. Aluminum can be incorporated controllably during epitaxial growth, or by ion implantation [3];
- can grow thermal SiO_2 with good electrical properties; ß-SiC MOSFETs have been successfully fabricated by various researchers [4,5].
- is not etched by HF; and
- can withstand temperatures up to 1400°C during homo/heteroepitaxial growth [6].

TABLE 1. KEYS' FIGURE OF MERIT FOR SELECTED SEMICONDUCTORS

Material	σ_T 300°K	V_{sat}	Dielectric Constant κ	$V_{sat}^{1/2}$ σ_T(---------) K	Ratio to Silicon
	(W/cm°C)	(cm/sec)	(Dimensionless)	($W/cm^{1/2}\ sec^{1/2}C$)	
Si	1.5	$1.0x10^7$	11.8	$13.8x10^2$	1
GaAs	0.5	$2.0x10^7$	12.8	$6.3x10^2$	.456
InP	0.7	$2.0x10^7$	14.0	$8.4x10^2$	.608
β-SiC	5.0	$2.5x10^7$	9.7	$90.3x10^2$	5.8

TABLE 2. JOHNSON'S FIGURE OF MERIT FOR SELECTED SEMICONDUCTOR MATERIALS

Material	E_B (volts/cm)	V_{sat} (cm/sec)	$\frac{E_B V_{sat}}{\pi}$ (volts/sec)	$P_M F_L^2 Z_L$ $\left(\frac{watt\text{-}\Omega}{sec^2}\right)$	Ratio to Silicon
Si	$3x10^5$	$1.0x10^7$	$9.5x10^{11}$	$9.0x10^{23}$	1.0
GaAs	$4x10^5$	$2.0x10^7$	$25.0x10^{11}$	$62.5x10^{23}$	6.9
InP	$6x10^5$	$2.0x10^7$	$38.0x10^{11}$	$144.4x10^{23}$	16.0
α-SiC	$40x10^5$	$2.0x10^7$	$250.0x10^{11}$	$6,250x10^{23}$	694.4
β-SiC	$40x10^5$	$2.5x10^7$	$320.0x10^{11}$	$10,240x10^{23}$	1137.8

In summary, the electrical properties of ß-SiC are outstanding and the chemistry of ß-SiC makes it very easy to work with existing silicon processing procedures. The *only* reason why ß-SiC has not yet been widely exploited in devices has been the unavailability of sufficiently large ß-SiC single crystals possessing semiconductor grade crystalline quality. Because ß-SiC is very refractory and does not melt congruently, efforts to directly synthesize ß-SiC have only produced small platelets [7]. The best way of creating semiconductor grade, monocrystalline ß-SiC is heteroepitaxial growth from a vapor [6].

1.2 Heteroepitaxial Growth of Semiconductor Grade ß-SiC

Research published by Parsons, Bunshah and Stafsudd [1] and by Parsons [6] has demonstrated that high quality ß-SiC can be heteroepitaxially grown on single crystal TiC_x substrates. The first paper described ß-SiC growth by reactive evaporation; the second paper described ß-SiC growth by chemical vapor deposition (CVD). In both cases, the resultant ß-SiC crystals had a very low density of stacking faults and other crystalline defects. It was pointed out that TiC_x is an excellent substrate for ß-SiC heteroepitaxial growth since TiC_x and ß-SiC have similar lattice constants and similar thermal expansion coefficients. At room temperature, the lattice constant of ß-SiC is 4.36 Å while the lattice constant of TiC is 4.33 Å. ß-SiC has zincblende structure while TiC has rocksalt structure. TiC_x can be nonstoichiometric and its lattice constant is a function of the carbon content, as illustrated in Figure 1. ß-SiC films grown on TiC_x float-zone crystals are suitably high quality for the fabrication of devices like MESFETS, MOSFETS and IMPATT diodes.

CVD processes generally can coat larger areas than PVD processes, so Parsons (of Hughes Malibu Research Laboratory) chose to grow ß-SiC on TiC_x by CVD. The paper by Parsons [6] discusses the problems associated with CVD growth. The optimal growth conditions listed in his paper were 5 sccm SiH_4, 0.2 sccm C_2H_4, 2 SLPM Ar and 0.9 SLPM H_2 at a growth temperature of 1400°C. Parsons noted that slight inequalities in the flow rates of SiH_4 and C_2H_4 resulted in the deposition of elemental carbon or silicon on the ß-SiC surface. Such unwanted deposits created poor morphology or even initiated polycrystalline growth. These fluctuations could not be arrested by mass flow controller technology. Therefore, Parsons concluded that *ß-SiC quality and yield would be improved using a source gas with Si and C present in a 1:1 stoichiometry.*

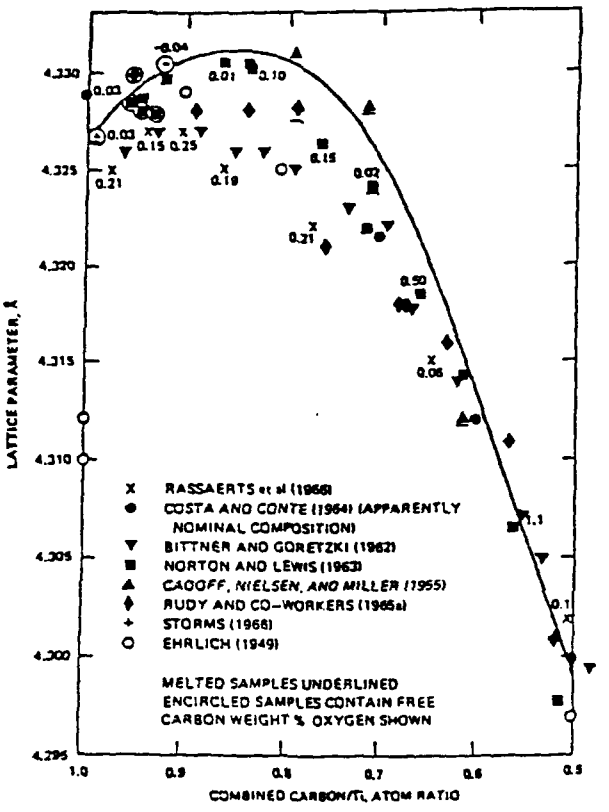

FIGURE 1. LATTICE CONSTANT OF TiC_x AS A FUNCTION OF CARBON/TITANIUM ATOM RATIO. (Reproduced from Reference 6).

2. PURPOSE OF THE RESEARCH

The purpose of this SBIR Phase I program was to grow heteroepitaxial ß-SiC on TiC substrates using two different source gases containing silicon and carbon in a 1:1 stoichiometry. DMI evaluated methylsilane, CH_3SiH_3, and methyl trichlorosilane (MTS), CH_3SiCl_3, as source gases for ß-SiC heteroepitaxial growth. Ideally, ß-SiC is deposited under the following reactions:

$$CH_3SiH_{3(v)} = ß\text{-}SiC_{(s)} + 3H_{2(g)} \quad (1)$$

$$CH_3SiCl_{3(v)} = ß\text{-}SiC_{(s)} + 3HCl_{(g)} \quad (2)$$

At 1500 K, the DG°_{rxn} of reaction 2 is -510 kJ/mol according to the JANAF Thermochemical Tables, 1985; hence, reaction 2 is highly favored toward complete reaction. (DG°_f data for methylsilane at 1500 K could not be obtained by DMI.)

The initial experimental procedure outlined in DMI's proposal was inspired by the paper published by Jim Parsons in the MRS Proceedings entitled Novel Refractory Semiconductors [6]. DMI discovered that some of Parsons' recommendations were very effective, while other suggestions produced poor results. At the beginning of the program, DMI followed the following recommendations of Parsons:

(1) ß-SiC was grown in a vertical flow reactor. Parsons stated that superior epitaxial films were grown from a vertical, cold wall CVD reactor whereby gases are introduced from the bottom and are exhausted from the top. The TiC substrate was suspended face down and was heated by a graphite susceptor. DMI designed and built its own version of such a reactor and found the inherent design philosophy to be sound. A major advantage of this design was that process gases encountered no solid objects between the inlet port and the substrate surface (except the 9 cm I.D. silica walls of the belljar). DMI also discovered that silicon carbide powder creation is unavoidable under all process conditions. The powder accumulated on the water-cooled container walls and along the sides of the susceptor. The vertical flow, face-down substrate geometry minimized powder accumulation on the substrate surface.

(2) Parsons recommended a specific procedure for polishing and cleaning and polishing TiC before use. This procedure was found to work quite well in producing very smooth TiC surfaces free of titanium oxide. DMI followed his procedure throughout the program.

(3) The TiC was carburized *in situ* preceding β-SiC growth. Parsons noted that TiC crystals made by the float zone process are carbon poor (nonstoichiometric). As illustrated in Figure 2, TiC_x possesses a wide range of carbon stoichiometries. The surface of a TiC crystal must be enriched with carbon immediately before growth of β-SiC. As discussed later, DMI developed procedures for *in situ* carburization of TiC (without graphite formation) in order to enhance the lattice match of TiC to the β-SiC.

(4) Parsons recommended the use of a pyrolytic boron nitride (PBN) pedestal as a container for the graphite susceptor and TiC substrate during epitaxial growth. This arrangement proved to be unsatisfactory for two reasons: (a) The white PBN rapidly became coated with dark SiC powder during a run. The SiC powder drastically increased the emittance of the susceptor assembly, resulting in severe temperature reduction. (b) Boron nitride chemically reacted with methyl trichlorosilane, producing powder thought to be NH_4Cl and/or Si_3N_4. Because of these problems, the use of the PBN pedestal was abandoned early in the research program.

(5) Parsons reported an optimal source gas composition of 5 sccm SiH_4, 0.2 sccm C_2H_4, 2 slpm and 0.9 slpm of H_2 at 1400°C. When this source gas mixture was compared to thermodynamic studies of β-SiC CVD [8,9], the thermodynamics indicated the mixture would produce a two phase deposit composed of β-SiC and silicon. In addition, DMI found that the use of *any* flow of argon resulted in co-deposition of silicon or graphite. The deleterious affects of argon diluent were supported by the thermodynamic studies. Therefore, the use of argon was discontinued for growth runs.

Additional inspiration from Jim Parsons (and co-workers G. Kruaval and J. Vigil) came from his talk delivered at ICACSC '88 in Santa Clara, CA, on December 15, 1988 [10]. Parsons pointed out that there is variability in the quality of TiC single crystals. The TiC crystals Hughes had grown contained pinholes and subgrain boundaries. β-SiC films heteroepitaxially grown on such crystals also contained pinholes and grain boundaries. The original TiC crystals used by DMI were very similar to the TiC described by Parsons. The quality of the TiC contributed to the poor morphology of the SiC films. During his talk, Parsons mentioned that the best β-SiC films he had ever produced were grown on TiC crystals synthesized by Mr. Walter Precht of Martin Marietta Laboratories in 1962. Two weeks after his talk in Santa Clara, Reznor Orr and Richard Koba of DMI contacted Mr. Precht and enlisted his assistance as a consultant to DMI. Mr. Precht supplied DMI with a monocrystalline boule of the alloy 95 mol% TiC + 5 mol% VC. The boule diameter was ≈1 cm. Wafers cut and polished from the boule were found to be free of pinholes and subgrain boundaries.

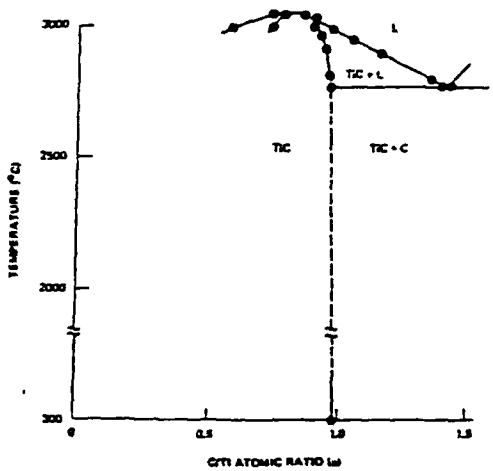

FIGURE 2. PARTIAL PHASE DIAGRAM OF THE Ti-C SYSTEM; NOTE THAT THE CONGRUENT MELTING POINT OF TiC_x OCCURS AT $X < 1$. (Reproduced from Reference 6).

Precht's carbide crystal was the substrate used by DMI to grow heteroepitaxial ß-SiC. DMI verified that the quality of the ß-SiC film is dependent upon the quality of the TiC substrate.

3. EXPERIMENTAL PROCEDURE

3.1 Design and Construction of the CVD Reactor

The ß-SiC reactor used was designed by a team composed of DMI's chief engineer, Ross Giammanco, electrical engineer, William Russell, materials scientist, Richard Koba, and the two consultants on this program, Dr. R. Bunshah and Dr. C. Deshpandey. The reactor is pictured in Figure 3. A dual wall, fused silica belljar was fabricated as a single unit; coolant water is passed through the two walls to maintain the inside wall near room temperature. The belljar is situated vertically and is surrounded by water-cooled copper induction coils connected to a 10 kW Lepel rf generator operating at a frequency of ≈ 450 kHz. The belljar incorporates several innovative designs to allow ease of use. The base of the silica belljar rests on a stainless steel baseplate containing a glass window pointed upward at the center of the belljar. Behind the window was placed a lens and fiber optic connected to a Mikron two-color optical pyrometer. The fiber optic bundle could be connected to a visible light source in order to accurately aim the pyrometer onto the surface of the TiC substrate.

TiC was placed in a susceptor assembly which was centered horizontally and vertically with respect to the induction coils. Gases were introduced through the baseplate via a 1/4" stainless steel tube whose aperture was directed at the surface of the TiC substrate. Gases were exhausted from the top of the belljar using a feed through cap which permitted the insertion of an alumina-clad thermocouple into the susceptor.

DMI's engineer, William Russell, designed and built an rf filter circuit to permit accurate reading of thermocouple temperature despite the rf induction field. Inside the susceptor, the thermocouple junction was separated from the TiC by less than 2 mm of graphite, permitting accurate measurement of TiC temperature under conditions of low flow rates of argon. The thermocouple was used to calibrate the optical pyrometer, permitting accurate correction for the emittance of TiC under the growth temperature regime, i.e., between 1200°C to 1400°C. After pyrometer calibration, actual CVD growth runs were run without the thermocouple in the susceptor to facilitate the changing of samples.

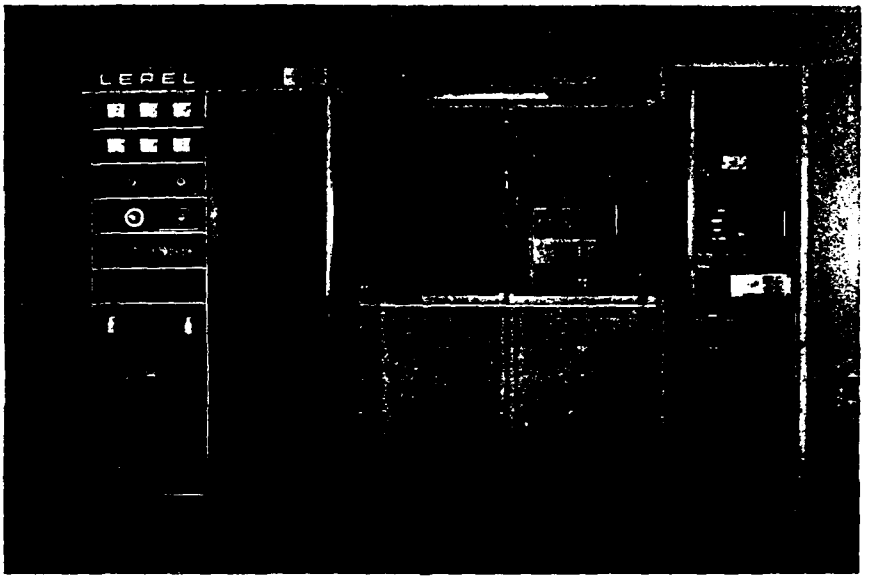

FIGURE 3. PHOTOGRAPH OF THE UPWARD, VERTICAL FLOW CVD REACTOR USED FOR THIS RESEARCH. This cold-wall CVD reactor was designed and built by Diamond Materials.

The CVD reactor pictured in Figure 3 was configured to run four process gases simultaneously. Argon was flowed through a mass flow controller of 2 slm capacity, hydrogen at 1 slm capacity, and ethylene, MTS or methylsilane were flowed through 100 sccm capacity mass flow controllers. The mass flow controllers were enclosed in the stainless steel box which was heated to a temperature of ≈ 35°C in order to discourage condensation of methyl trichlorosilane. Under 1 atm pressure MTS has a boiling point of 66°C.

SiC was deposited using methylsilane as well as methyl trichlorosilane. The CH_3SiCl_3 was purchased from Advanced Technology Materials and was assumed to be > 99.9% pure. ATM supplied a stainless steel bubbler which had dual capabilities of running a purge gas or carrier gas as necessary. Pure MTS was flowed through its mass flow controller in order to enhance the accuracy of MTS flow and promote good reproducibility. The MTS stainless steel bubbler was placed in a steel container and heated to a sufficient temperature near 60°C to insure steady flow through the mass flow controller into the belljar.

DMI had difficulty discovering a vendor for methylsilane. After a diligent month-long search, it was discerned that the only domestic vendor of methylsilane is Petrarch Systems of Bristol, PA. DMI was able to purchase this gas in a steel, compressed gas cylinder. However, it took Petrarch Systems over two months to fill the order. The purity of the methylsilane was not as good as the methyl trichlorosilane bought from ATM. Petrarch Systems could only guarantee a purity no less than 97%.

Another unique feature of DMI's reactor was the use of a novel throttle valve. This throttle valve was developed for DMI by a noted vendor of pressure control equipment. The throttle valve permitted the attainment of any required pressure from atmospheric down to ≈ 1 torr. This throttle valve was quite useful in optimizing the total pressure for β-SiC growth. At atmospheric pressure, growth of β-SiC tended to produce large quantities of powder and increased convective heat losses from the susceptor. Pressures below 200 torr tended to produce plasmas inside the chamber, even in the presence of pure hydrogen. Therefore, stable processing was carried out at 250 torr.

DMI's reactor also included various safety features. The fused silica belljar was enclosed in a steel cabinet with hinged doors and plexiglass viewports. Methylsilane and methyl trichlorosilane were operated in a gas manifold which could be purged with argon. Hazardous gas sensors were placed inside the steel chamber surrounding the silica belljar as well as in the gas cylinder cabinet containing the methylsilane cylinder. Electronic interlocks ensured that the silica belljar had to be evacuated by the

vacuum pump immediately at the start and after the completion of any process run. The chamber was vented with dry nitrogen after each run. Effluent gas was pumped by an Alcatel chemical series rotary pump fitted with Fomblin oil. Effluent from the Alcatel pump was then directed to a multichamber, gas scrubber with automatic pH control system.

3.2 Evolution of the Susceptor Design

Figure 4 contains schematic diagrams of the three susceptor designs employed throughout the research. The original susceptor design was inspired by a paper published by Jim Parsons [6]. As described by Parsons, the TiC is situated face down in a hole created in a pyrolytic boron-nitride pedestal. A graphite susceptor rests on the back face of the TiC substrate and is responsible for heating the TiC to temperatures of at least 1400°C. Source gases pass between the inside wall of this water-cooled silica belljar and the effluent orifice. DMI's original susceptor assembly design is illustrated in Figure 4a. A pyrolytic boron-nitride pedestal was created whose length equaled the length of the induction coils, i.e., ≈ 12 cm. The top of the boron-nitride pedestal was suspended above the top of the induction coils by three stainless steel wires and a ring assembly at the top of the belljar. A graphite susceptor was placed in contact with the back of the TiC substrate inside the boron-nitride pedestal. The original design could achieve temperatures in excess of 1350°C. Despite the large area of the graphite susceptor, radiation losses were reduced by the white pyrolytic boron-nitride pedestal. However, use of the pyrolytic boron-nitride pedestal was found to cause two problems:

(1) SiC growth from mixtures of methylsilane and ethylene inevitably resulted in the deposition of dark SiC powder on the surface of the pyrolytic boron-nitride pedestal. Such deposition dramatically increased the emittance of the pyrolytic boron nitride pedestal resulting in a temperature drop up to 200°C after a 60 minute run.

(2) It was found the pyrolytic boron-nitride chemically reacted with methyl trichlorosilane at growth temperatures. Powder formation was so severe that the throttle valve became clogged and inoperable. Because of this, the pyrolytic boron-nitride pedestal was no longer used.

The pyrolytic boron-nitride pedestal was replaced by a similar graphite one. However, this design proved to be ineffective because of the extremely high emittance of graphite. Radiation losses prevented this replacement assembly to achieve any

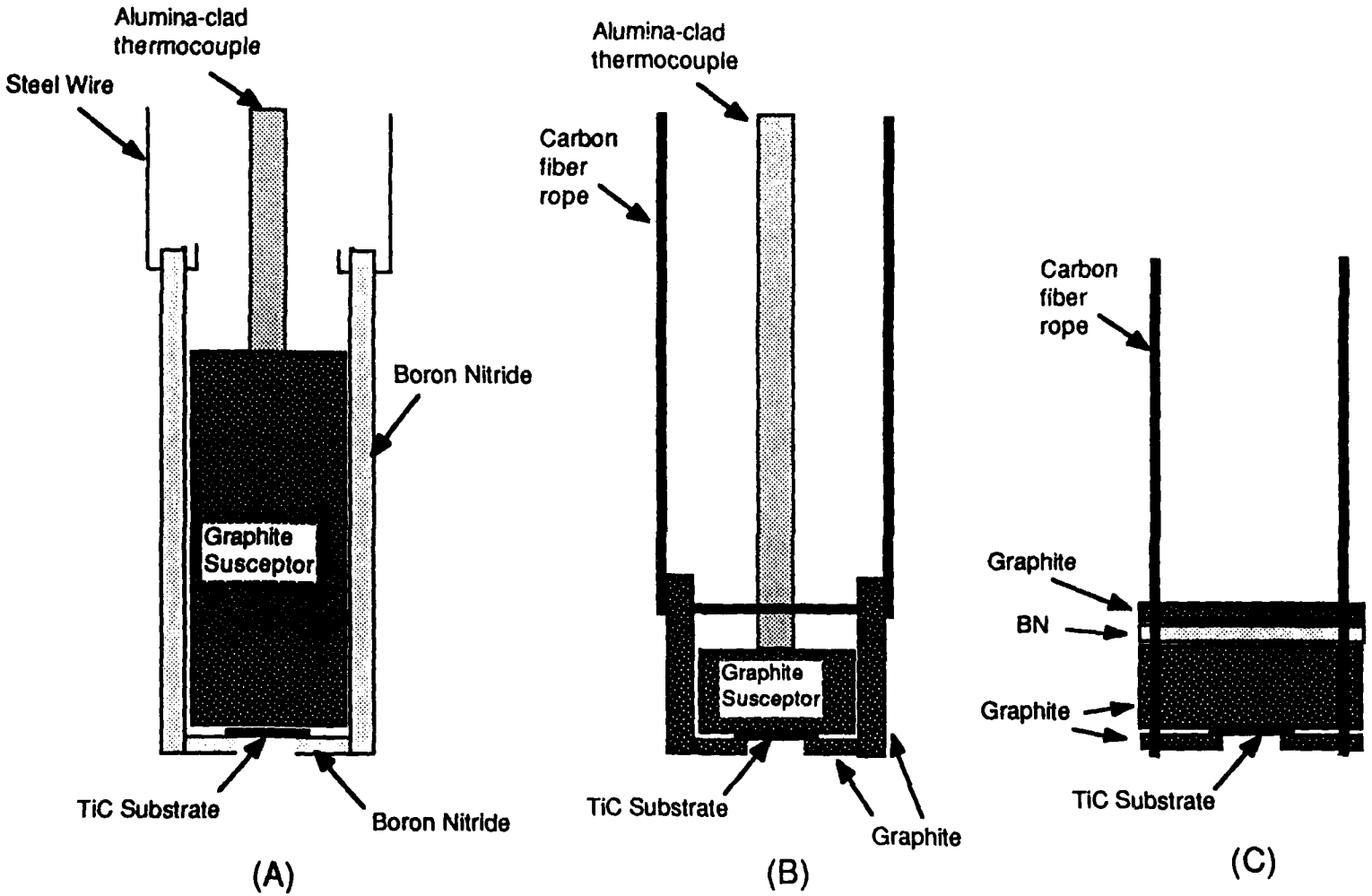

FIGURE 4. SCHEMATIC DIAGRAM OF THE THREE SUSCEPTOR ASSEMBLIES USED DURING THE RESEARCH PROGRAM. (A) Initial design included a pyrolytic boron nitride pedestal ; (B) second design included a carbon fiber rope to suspend the susceptor in the middle of the induction coils; (C) final design achieved temperatures above 1400°C.

temperature above 1100°C. At that point, DMI realized that the goal was to achieve a much smaller surface area graphite susceptor placed within the center of the induction coils with a minimum of surface area to minimize radiative heat loss. However, it was impossible to extend the stainless steel wires down into the susceptor region because the steel wire would couple and melt.

SiC and then ultimately, carbon graphite fiber rope was used in order to suspend the graphite assembly inside the middle of the induction coils. Tyranno and Nicalon (brands of SiC fibers) were initially found to be chemically reactive and unable to be used longer than one run. More conventional carbon graphite fibers were used and found to be much less chemically reactive than the SiC fibers. Since the carbon fibers did not couple with the rf field, the only part of the carbon fibers which became hot was the portion in contact with the graphite susceptor. The carbon fibers could also be easily handled and maintained their integrity at temperatures well over 1400°C. The result was the susceptor assembly illustrated in Figure 4b in which carbon graphite fibers were looped through the top of a pedestal assembly. The maximum temperature achieved by the situation illustrated in Figure 4b was only 1300°C. Such low deposition temperature produced polycrystalline ß-SiC films, therefore, it became obvious that much higher deposition temperatures would have to be achieved and sustained throughout a long deposition run in order to promote heteroepitaxial growth of ß-SiC the TiC substrates.

DMI developed the third susceptor design illustrated in Figure 4c. This design used stacked layers of graphite and boron-nitride in order to maximize coupling efficiency yet minimizing radiative losses. The key feature of this successful design was the use of a boron-nitride plus graphite cap. Most of the coupling was on the middle graphite disk. Radiation losses through the top of this disk were minimized by a placement of a thin boron-nitride disk of equal area on top. However, this boron-nitride had to be shielded from the methyl trichlorosilane to prevent powder deposition, so a thin graphite wafer was placed atop the boron-nitride. The susceptor illustrated in Figure 4c was used to attain temperatures above 1400°C during extended growth runs. This susceptor was the one which permitted heteroepitaxial growth on monocrystalline ß-SiC.

3.3 TiC Substrate Preparation

DMI discovered, as did Parsons [6], that preparation of the TiC substrate is absolutely critical in order to achieve (a) growth of single phase ß-SiC, and (b)

monocrystalline growth. To be suitable for β-SiC heteroepitaxy, TiC substrates had to be prepared both physically and chemically. Physical preparation refers to polishing and cleaning the substrates in order to obtain a carbide surface flat, smooth, free of scratches, and free of oxide contamination. Chemical preparation refers to the achievement of a stoichiometric TiC surface which is monocrystalline and free of graphite inside the reactor immediately before the onset of β-SiC deposition.

3.3.1 Physical Preparation of TiC Substrates

DMI followed the procedure for preparation of TiC recommended by Parsons. The identical procedure was followed for the pure TiC samples supplied by Bunshah and Deshpandey of UCLA, as well as the (Ti,V)C boule supplied by Walter Precht of Martin Marietta. Both samples are illustrated in Figure 5. Bunshah and Deshpandey supplied DMI with small samples of pure TiC which were already polished. Precht supplied DMI with a portion of a boule of 95 mole % TiC plus 5 mole % VC. The boule was supplied with one surface cut and polished along the {100} orientation. This surface orientation had been measured at Martin Marietta by Laue diffraction. At DMI, the sample was cut into slices parallel to the {100} face with a diamond wafering saw.

All carbide substrates were then polished using a series of fixed diamond abrasive papers. Grinding was performed using 15, 9, 6, 3, and 1 μm diamond abrasives in sequence. The sample was then rinsed in methanol. After characterization by SEM and Raman, sample SiC films were routinely removed by grinding and polishing in order to re-use the valuable TiC substrate.

After the grinding operation, a chem/mechanical polish was performed [6]. A solution was prepared composed of

1. 45 g of $K_3Fe(CN)_6$,
2. 1 g of KOH,
3. 200 cc of water, and
4. 0.5 g of submicron diamond powder.

Droplets of the solution were placed on a felt polishing cloth and the TiC was hand polished for one minute. The sample was then cleaned in room temperature methanol in an ultrasonic bath for one minute. Following the methanol rinse, the sample was then etched in a solution of 2:8 HNO_3:H_2SO_4 for two minutes at room temperature. This step was recommended by Parsons in order to remove an outer layer of titanium

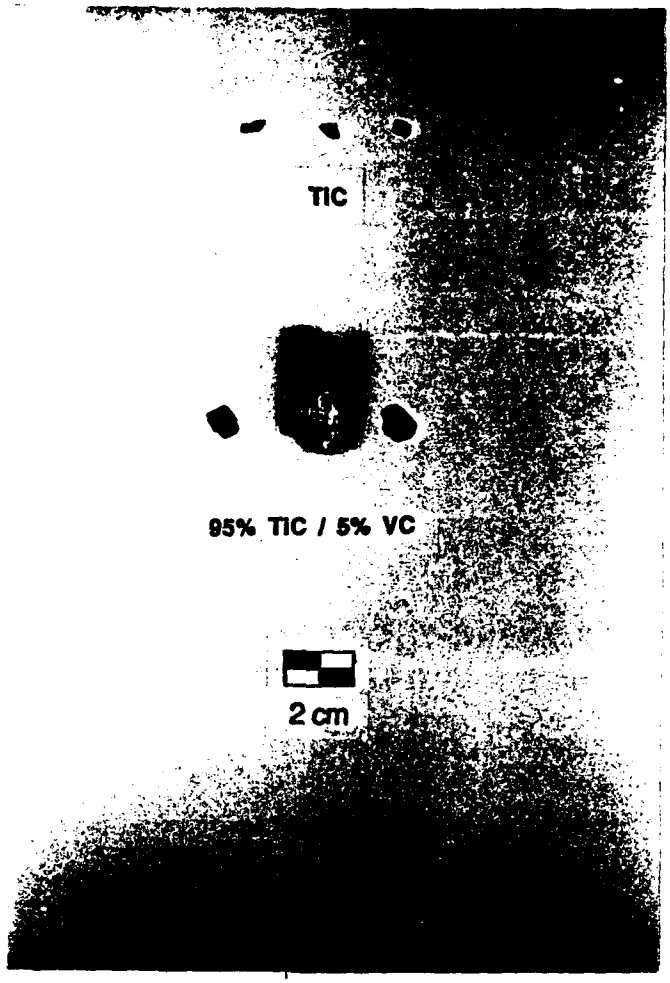

FIGURE 5. PHOTOGRAPH OF THE SUBSTRATES USED FOR THIS RESEARCH PROGRAM. The samples on top are the pure TiC crystals obtained from Bunshah and Deshpandey. These samples contained pinholes and may have contained subgrain boundaries. The samples on the botton are slices and the boule obtained from Walter Precht. The composition of the bottom crystals is 95 mol % TiC + 5 mol % VC.

oxide as well as etch a few layers of TiC. Following this etch, the sample was thoroughly rinsed in distilled water and methanol. The sample was then immediately loaded in the CVD susceptor face down. An SEM of a micrograph of a smooth sample provided by Walter Precht is shown in Figure 6. As predicted by Parsons, this chem/mechanical polishing procedure indeed produces films which are smooth even under SEM observation.

3.3.2 Chemical Preparation of TiC

The correct *chemical* preparation of TiC substrates prove to be the critical processing step which enabled growth of heteroepitaxial β-SiC. As shown in Figure 2, TiC has a wide range of carbon stoichiometries. As shown in Figure 1, the lattice constant of TiC varies as a function of C/Ti atomic ratio. Parsons pointed out that all float zone samples of TiC are carbon poor with stoichiometries around $TiC_{.85}$. To grow heteroepitaxial β-SiC, the TiC substrate surface must be composed of single phase, monocrystalline TiC with a carbon rich stoichiometry at the growth temperature, immediately before and throughout β-SiC growth. DMI discovered that achieving the correct TiC surface chemistry is not trivial because SiC CVD occurs in a hydrogen-rich ambient at temperatures above 1200°C.

DMI had to develop a procedure to heat the TiC to the growth temperature and carburize it in a hydrocarbon ambient in order to prevent: (a) etching of the TiC, (b) formation of any amorphous phases, or (c) deposition of graphite from the carburizing ambient. Two sets of carburizing experiments were performed. Each set of experiments was targeted to the different growth temperature. The substrate susceptor illustrated in Figure 4b could only achieve temperatures up to around 1310°C for a limited time. Therefore, a carburization procedure was developed at the temperature 1250°C. Carburization was achieved by heating the sample in pure hydrogen and then exposing the TiC to a mixture of ethylene and hydrogen at 1250°C for 10 minutes.

The key to carburization was to discover an ethylene/hydrogen ratio high enough to saturate the TiC_x surface to a stoichiometry near TiC_1 without condensing graphite. Graphite deposition occurred according to the following reaction:

$$C_2H_{4(v)} = 2C_{(s)} + 2H_{2(g)} \qquad (3)$$

At 1500 K, the $DG°_{rxn}$ of reaction 3 is -160.3 kJ/mol at 1 atm pressure. The carbon phase is graphite. If hydrogen is assumed to be fixed at an activity of 1 (since hydrogen

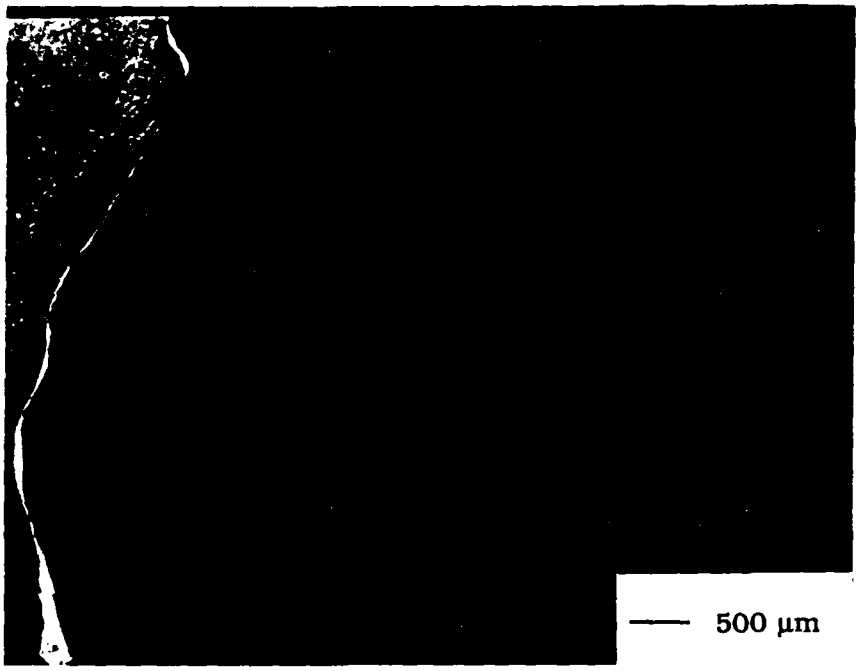

FIGURE 6. SEM MICROGRAPH OF (Ti,V)C SUBSTRATE RECEIVED FROM W. PRECHT.

is used as the diluent), then the equilibrium activity of ethylene is calculated to be 2.6 x 10^{-6}. However, hydrocarbons, especially in the presence of high hydrogen dilution are notorious for their inability to achieve the thermodynamically predicted concentrations in an open, free flowing CVD reactor.

A series of experiments was performed carburizing bare TiC substrates at various relative flows of ethylene and hydrogen. First at 1 slm of hydrogen, the ethylene content was varied between 1, 2, and 5 sccm. Immediately following the flow of ethylene at a temperature of 1250°C, the sample was returned to room temperature and examined by Raman spectroscopy. It was found by Raman that graphite formation occurred at a flow rate of 5 sccm but was absent in the 1 and 2 sccm samples. Therefore, all SiC growth runs were immediately preceded by a carburization at 1250°C for 10 minutes in 0.2% C_2H_2 /H_2. Raman analysis of these samples produced no notable Raman response since the Raman spectrum of monocrystalline TiC, regardless of stoichiometry, is insignificant. Carburization at 1250°C also did not produce any noticeable etching of the TiC. Since the carburization procedure developed at 1250°C was very effective in producing an appropriate TiC surface, single phase β-SiC films were easily grown at temperatures below 1300°C.

However, SiC growth experiments at temperatures 1300°C and lower were discontinued because monocrystalline β-SiC could not be deposited. As discussed in Section 5, various research papers report that such a low deposition temperature supplies insufficient surface atom ability to the Si and carbon atoms during growth; therefore, only polycrystalline β-SiC films were observed.

After it became evident that monocrystalline TiC could not be achieved at temperatures below 1300°C, the susceptor assembly illustrated in Figure 4c was created which enabled the routine achievement of temperatures of 1400°C. The first β-SiC growth runs attempted at 1400°C utilized the 1250°C carburization procedure, since it was assumed that the TiC surface chemistry would not be affected during the two minute ramp from 1250°C to 1400°C. However, analysis of the film produced using this procedure indicated that the TiC substrate was altered radically by the ramp from 1250°C to 1400°C in hydrogen. Contrary to expectation, β-SiC was not observed by Raman spectroscopy on the sample. Instead, the surface was covered with an amorphous phase whose Raman spectrum had two, broad peaks. The amorphous phase appeared flaky on the TiC surface. The conclusion was reached that the carburization procedure at 1250°C was completely inadequate to support SiC growth at 1400°C. The chemistry of the TiC surface became drastically different at 1400°C than at 1250°C.

Before further β-SiC growth experiments could be performed, a thorough set of TiC carburization experiments were performed at 1400°C. The dissociation of ethylene at 1700 K is described in reaction 3 has a $DG°_{rxn}$ of -177 kJ/mol. Under atmospheric pressure and unity activity of hydrogen, the activity of ethylene in equilibrium with graphite is 3.6×10^{-6} which is similar to ethylene's equilibrium activity at 1500 K. Since thermodynamics did not accurately predict the correct percentage of ethylene necessary for 1250°C carburization, DMI methodically studied the carburization of TiC at 1400°C. The experimental procedure was as follows:

1. A TiC crystal was polished, etched, and cleaned according to the procedure described in Section 3.3.1.
2. The crystal was loaded into the reactor and the selected ratio of ethylene to hydrogen was flowed, starting at room temperature.
3. The sample was ramped in temperature from room temperature to 1400°C in eight minutes and was then soaked at 1400°C for 30 minutes. After 30 minutes, temperature ramped to ≈ 600°C within 4 minutes. At 700°C the ethylene flow was cut and further cooling was performed in an ambient of pure hydrogen.

Seven different mixtures of ethylene and hydrogen were run and after each growth run, the TiC surface was observed by optical microscopy and the Raman spectrum of the surface was collected. As discussed in the results section, the TiC surface structure and chemistry varied radically as a function of the ethylene content during the carburization procedure. All carburizations were performed at a total pressure of 250 torr.

3.4 β-SiC Deposition

The beginning of a typical SiC growth run followed the optimal *in situ* carburization step. Immediately following the carburization step, the ethylene was turned off and replaced with the source gas mixture used for β-SiC deposition.

One of the first issues which needed to be resolved was the total pressure necessary to grow β-SiC. At first, all β-SiC growth runs were performed at a pressure of 700 torr, just under atmospheric pressure. Operation at exactly atmospheric pressure was not possible due to the continuous use of the mechanical vacuum pump. Pressure was maintained by the use of an innovative throttle valve located between the belljar and the mechanical pump. In order to prevent overpressure of the belljar and possible

explosions, a pressure interlock was installed which would immediately cut gas flow if the pressure ever exceeded 730 torr. Therefore, 700 torr was selected to provide a comfortable margin for error in case of transient pressure increases.

Several early runs using methylsilane and MTS were performed at 700 torr. However, it was observed that the use of this high pressure (1) promoted the formation of SiC powder on the susceptor and on the inside walls of the silica tube, and (2) seemed to promote temperature loss of the sample due to convective heat loss by the high-pressure flowing gas. Therefore, it was decided to perform all growth runs at a lower pressure. The low pressure operation limit seemed to be 200 torr since at this pressure or below, formation of plasma was observed by the rf field, even under pure hydrogen ambients. Therefore, most growth runs were performed at a total pressure of 250 torr which mitigated formation of powder and convective heat loss, yet prevented plasma formation.

Original growth runs were performed using mixtures of methylsilane mixed with ethylene. For reasons to be discussed in Section 5, the ethylene/methylsilane mixture was controlled in order to insure C/(C + Si) ratio of 0.4. This elemental ratio in the source gas mixture ensured formation of single phase ß-SiC as predicted by thermodynamics. The methylsilane source gas was supplied from a pressurized cylinder through a regulator into a mass flow controller. DMI did not independently measure the purity of this source gas, nor were any further steps taken to purify the gas between the gas cylinder and the belljar.

Methyl trichlorosilane (MTS) was supplied from a stainless steel bubbler. Both the bubbler and the MTS were supplied by Advanced Technology Materials and had purities in excess of 99.9%. The MTS stainless steel bubbler had a valve system which permitted purging of the feed lines, the use of a carrier gas, or the direct output of MTS in its pure vapor state. DMI elected to use pure MTS since its flow rate could be accurately controlled by a mass flow controller.

Since MTS has a boiling point of 66°C, DMI discovered that the inherent vapor pressure of MTS at room temperature was unable to support a sufficient stream from the bubbler through 50 cm of stainless steel tubing into the mass flow controller and then through an additional 25 cm of tubing into the glass belljar. All mass flow controllers used for this research program were enclosed in a box which was heated to a temperature of ≈ 40°C. A hotter temperature mass flow controller than source gas did not promote the flow sufficient MTS, therefore, the MTS was heated to a temperature near 60°C in order to supply sufficient pressure to allow the MTS to flow from the

reservoir and through the mass flow controller into the belljar. The stainless steel lines between the reservoir and mass flow controller were heated to 30°C with heat tape.

Essentially, two different growth procedures were used depending on the susceptor used. With the susceptor illustrated in 4b, temperatures only between 1250 and 1300°C could be achieved. The total growth procedure was typically as follows:

1. TiC sample was prepared and then inserted according to the procedure outlined in Section 3.3.
2. The sample was heated with a pure hydrogen ambient from room temperature up to 1250°C within 8 minutes.
3. Carburization was performed using 10 sccm ethylene + 1 slm of hydrogen at 1250°C for 10 minutes.
4. The ethylene was turned off and the temperature ramped to the highest possible temperature attainable by the current susceptor design. Typically this temperature was between 1325 and 1350°C.
5. After achievement of temperature, the methylsilane + ethylene mixture or MTS was then turned on and the run continued for 2 to 3 hours.
6. After completion of the run, the β-SiC source gas was then turned off and the sample was allowed to cool to room temperature in a pure hydrogen ambient during a ramp down time of approximately 10 minutes.

After the susceptor design shown 4c was instituted, permitting attainment of temperatures of 1400°C, the following procedure was then followed:

1. The TiC sample was polished, cleaned, and rinsed according to procedure outlined in Section 3.3.
2. The sample was loaded into the susceptor. The reaction chamber was evacuated to below 1 torr for 5 minutes and then 12 sccm of ethylene + 1 slm of hydrogen were let into the chamber until the total pressure of 250 torr was achieved.
3. Temperature ramp-up then occurred from room temperature to 1400°C in ≈ 8 minutes.
4. TiC was carburized at 1400°C for 30 minutes.
5. The ethylene was immediately turned off and the methyl trichlorosilane was turned on for a growth run 10 to 30 minutes in duration.
6. The MTS flow was then terminated and the sample was allowed to cool to room temperature in an ambient of 1 slm hydrogen.

7. The hydrogen flow was turned off and the belljar was evacuated, then vented with pure nitrogen before removing the sample.

It is important to point out that this latter procedure was not developed until the supply of methylsilane had been exhausted. Therefore, this latter procedure was performed only using MTS. However, DMI feels that the combination of methylsilane and ethylene would probably have also been effective in growing SiC by the second procedure. Of course, it was the second procedure which was used to grow heteroepitaxial β-SiC.

3.5 Film Characterization

After each sample was removed from the reactor, it was examined with a Ramanor U1000 microfocus Raman spectrometer. This spectrometer was equipped with an Olympus optical microscope. A color television camera was connected to the optical microscope to permit viewing of the sample surface on a color monitor. Surface morphology was inspected at 50 and 100X magnification. Microfocus Raman analysis was also performed through the optical microscope; the laser light as well as the scattered Raman light were conducted through microscope optics.

In order to perform accurate qualitative analysis, DMI obtained well-characterized samples of α-SiC, α+β-SiC, graphite, and silicon. Raman spectra of these samples were collected in order to create a reference library. The Raman spectrum of monocrystalline silicon graphite, in α-SiC crystal grown by the Acheson process and of an industrial, polycrystalline CVD SiC film are shown in Figures 7-10, respectively. The industrial CVD film is shown to be a mixture of α-SiC and β-SiC. This spectrum was compared to published Raman spectra of pure α-SiC and β-SiC. As shown in Figure 11, the 6H polytype of α-SiC has strong Raman peaks at 789 cm^{-1} and 967 cm^{-1} while β-SiC (a.k.a. 3C-SiC) has a weaker Raman response, with peaks at 796 cm^{-1} and 972 cm^{-1}. The pure TiC substrates were also analyzed by Raman spectroscopy as well as the 5% VC/TiC alloy. In both cases, the carbide crystals were found to have insignificant Raman response (as is true for most crystals of rocksalt structure). Figure 12 is a Raman spectrum of pure TiC.

Known Raman spectra were used in the identification of most phases produced during the experiments of this research program. Raman spectroscopy proved to be extremely valuable since it was used not only for characterization of as-deposited SiC films, but it was also used to characterize the TiC surface after the carburization

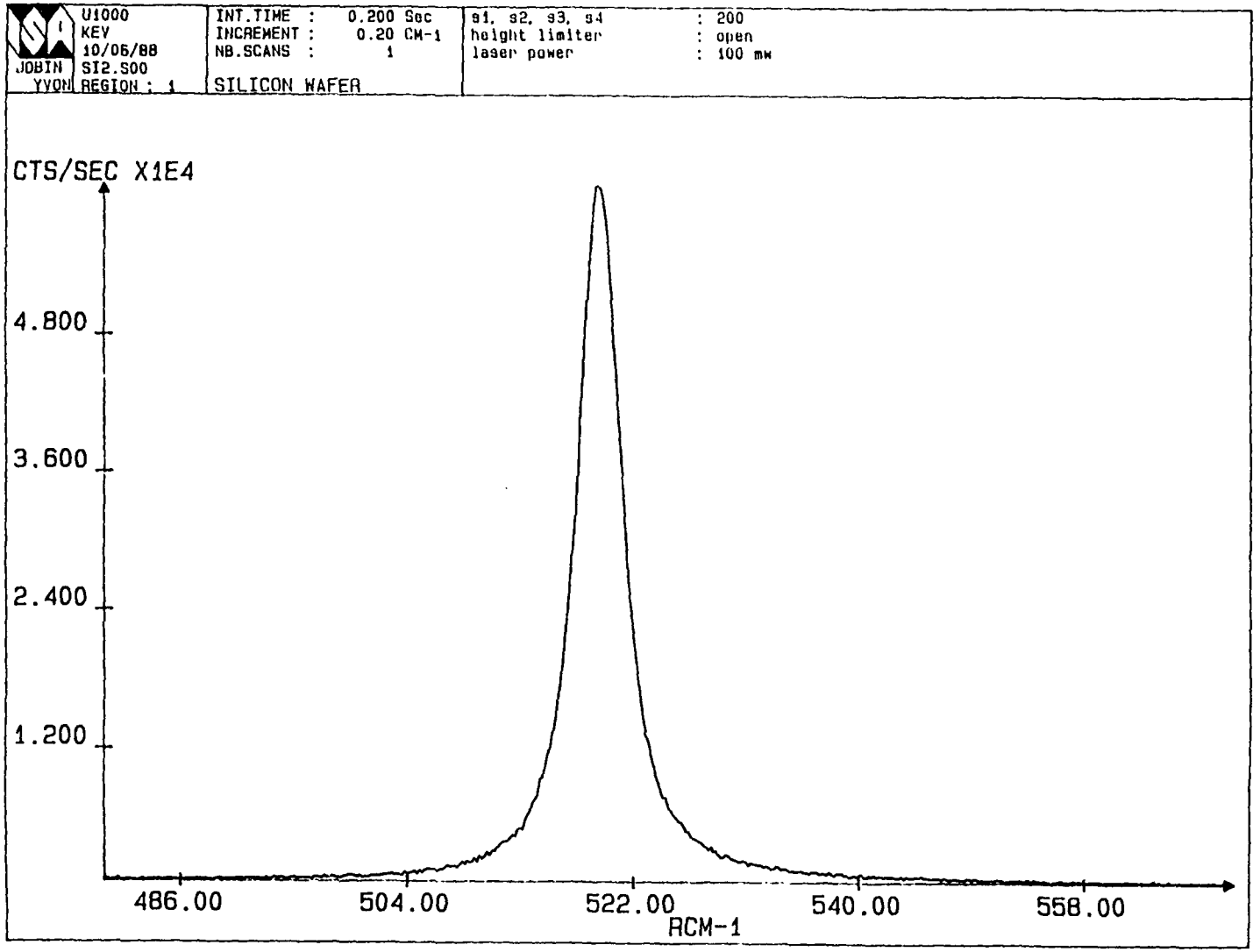

FIGURE 7. RAMAN SPECTRUM OF SILICON.

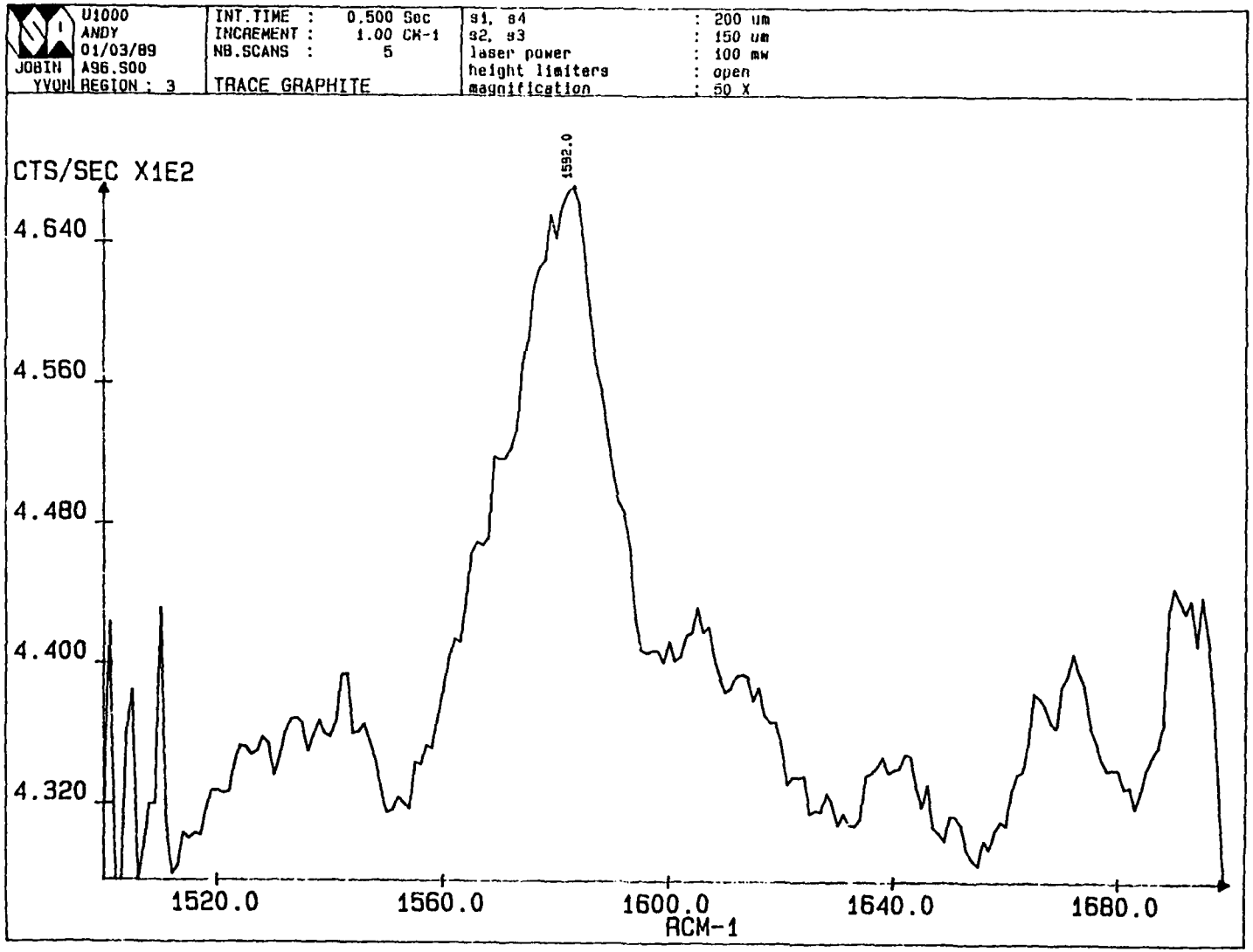

FIGURE 8. RAMAN SPECTRUM OF GRAPHITE.

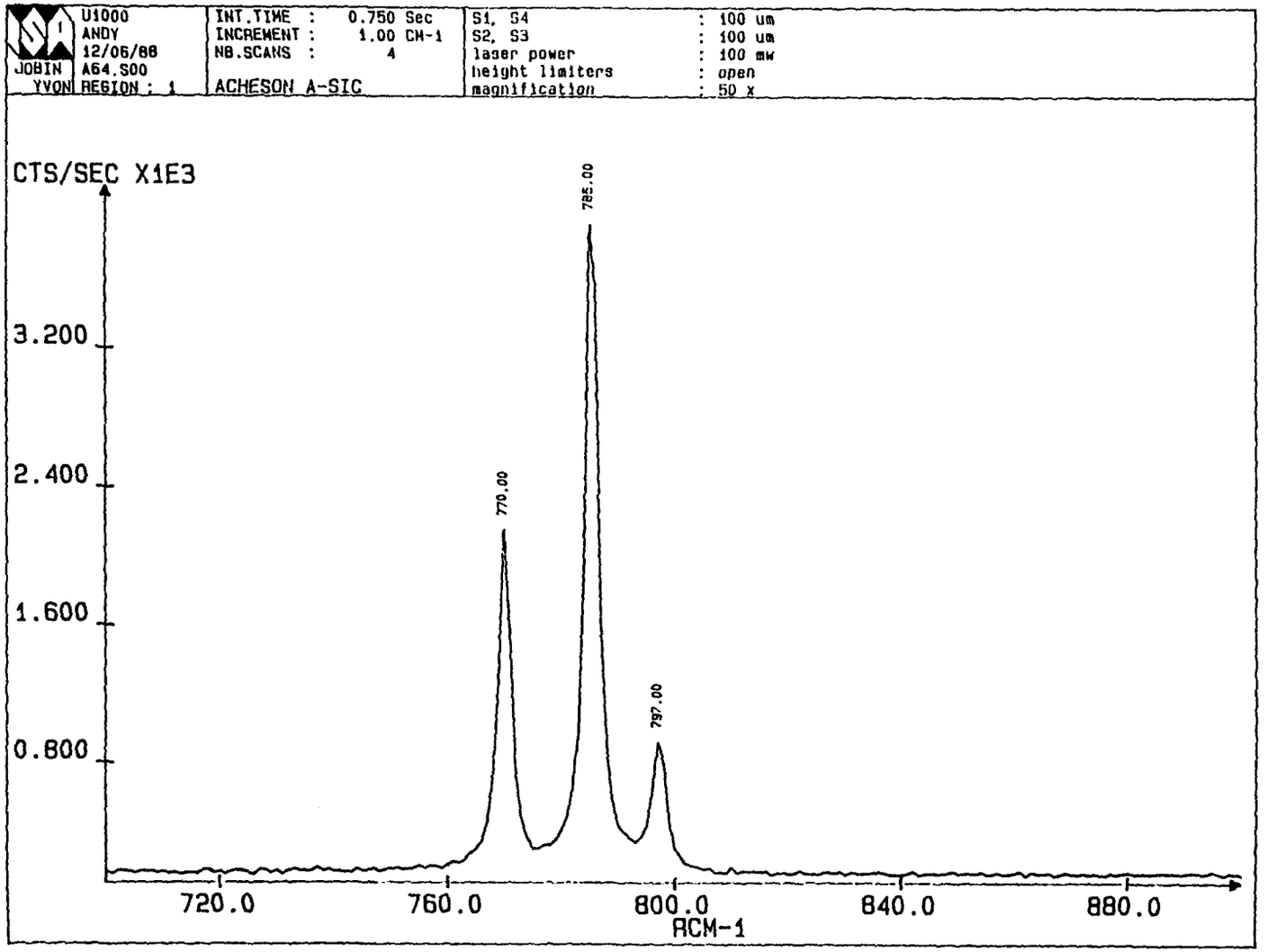

FIGURE 9. RAMAN SPECTRUM OF A α-SiC CRYSTAL MADE BY THE ACHESON PROCESS.

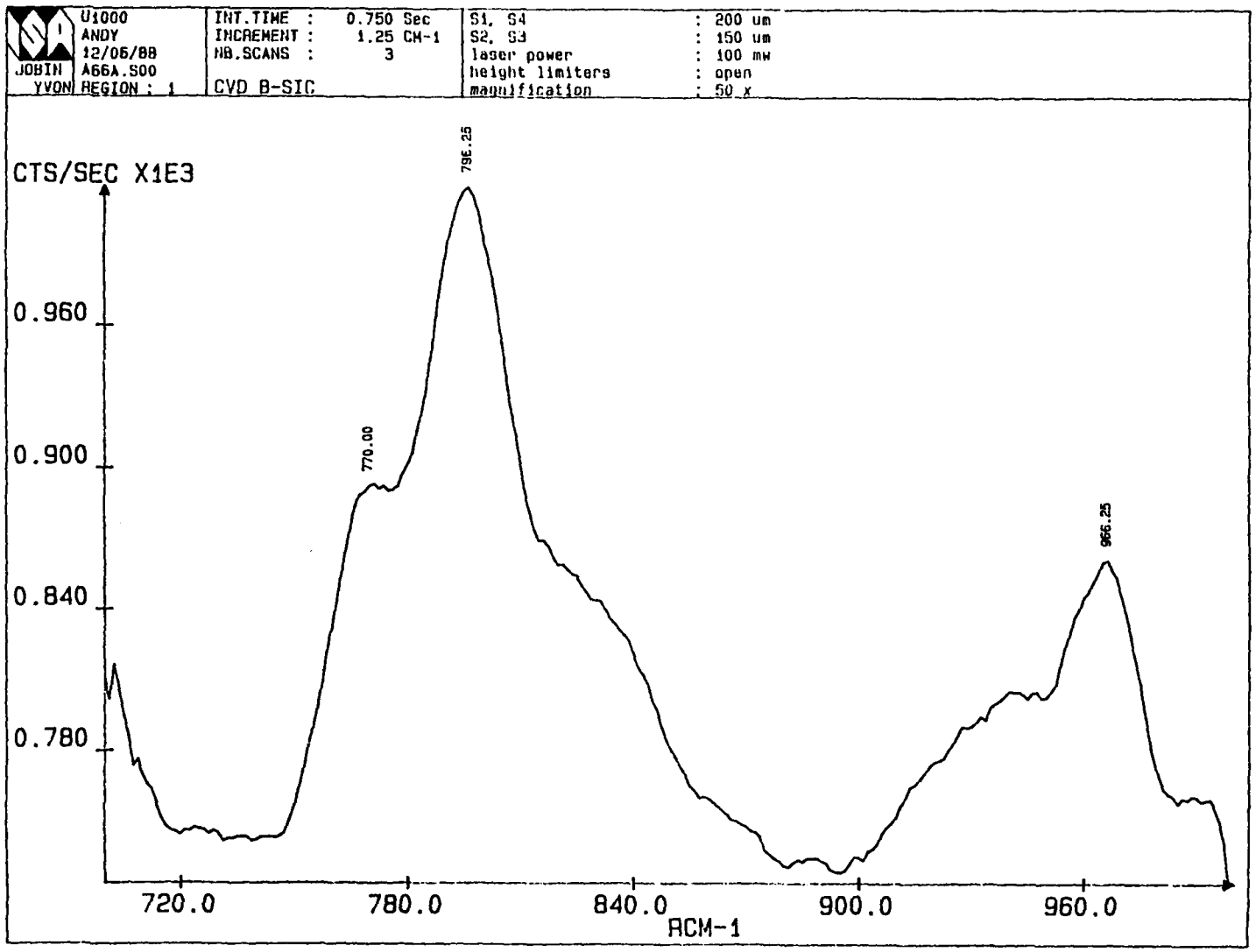

FIGURE 10. RAMAN SPECTRUM OF AN INDUSTRIAL, POLYCRYSTALLINE CVD SiC FILM. The film contains both α-SiC and β-SiC.

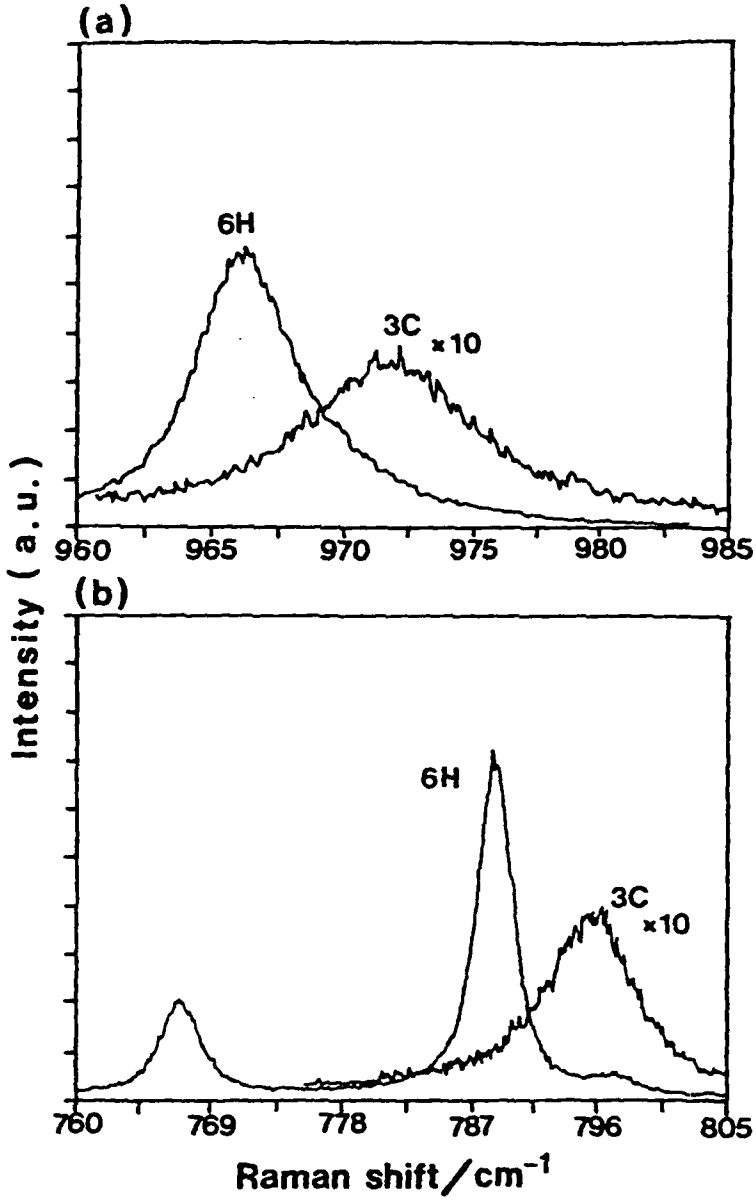

FIGURE 11. RAMAN SPECTRA OF 6H SiC AND 3C -SiC (β-SiC). Spectrum (a) covers the region from 960 to 985 cm^{-1}, while (b) covers the region from 760 to 805 cm^{-1}. (Reproduced from H. Okumura, E. Sakuma, J. H. Lee, H. Mukaida, S. Misawa, K. Endo and S. Yoshida, "Raman Scattering of SiC: Application to the Identification of Heteroepitaxy of SiC Polytypes," *J. Appl. Phys*, 61 [3] 1134 (1987)).

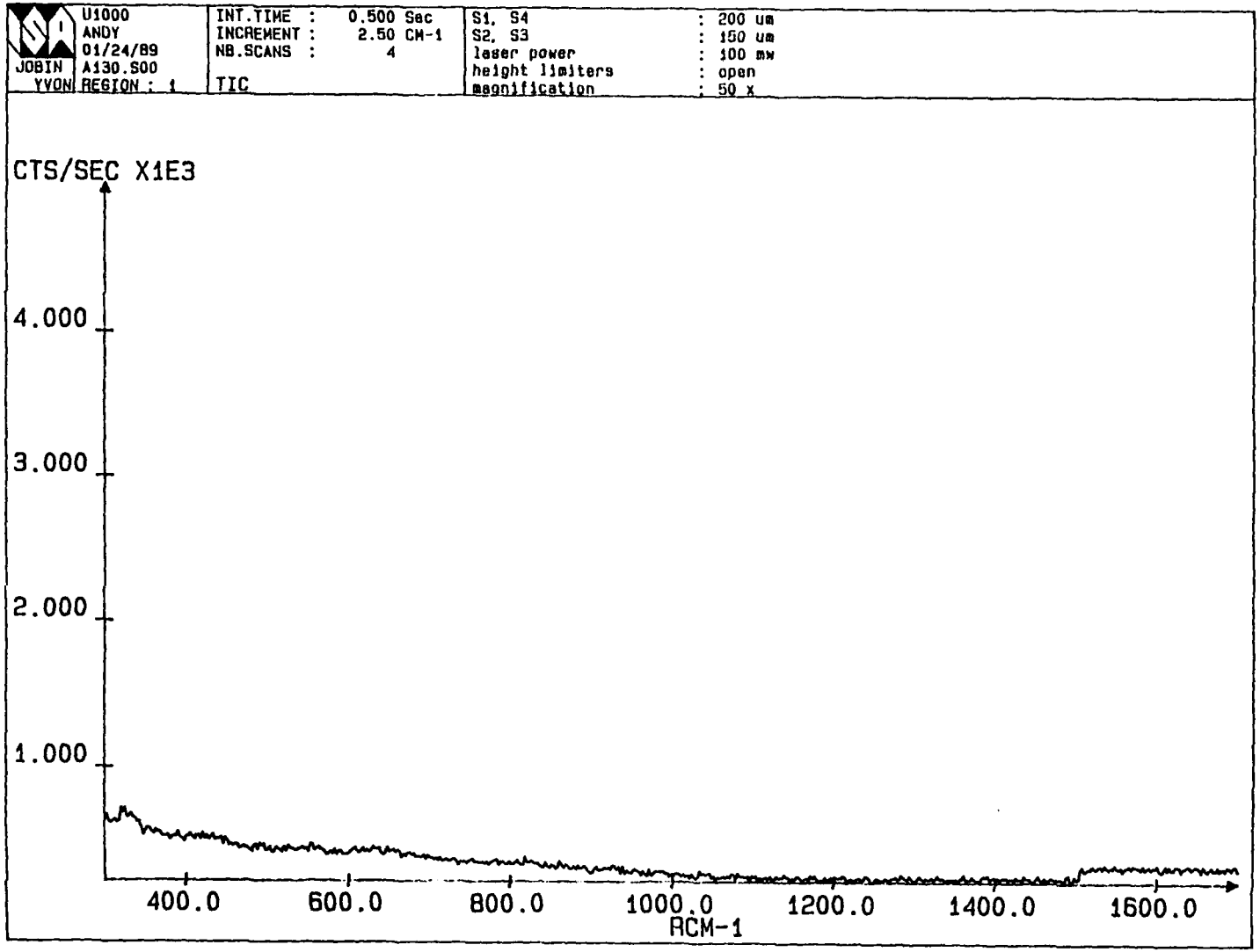

FIGURE 12. RAMAN SPECTRUM OF A TiC SINGLE CRYSTAL.

experiments. Raman spectroscopy is especially sensitive to graphite, so carburization experiments were performed until a carbon-saturated, crystalline TiC surface was obtained which was free of any graphite. Such a stoichiometric, yet graphite-free surface was the key to nucleating a monocrystalline, β-SiC film.

After Raman spectroscopy, selected films were imaged by scanning electron microscopy using *ISI* SEMs at Penn State University. Because of the electrically conducting nature of the TiC and the SiC, it was unnecessary to carbon or gold coat any samples before SEM analysis. Once a flat and smooth SiC film had been produced, the sample was submitted for analysis by cross-sectional SEM.

4. EXPERIMENTAL RESULTS

4.1 Carburization Experiments

As described in Section 3, DMI performed two sets of carburization experiments. One set of carburization was performed at 1250°C, while the other set was performed at 1400°C. Carburization at 1250°C was performed with 1 slm of H_2 and 1, 2, and 5 sccm of C_2H_4; the carburization time was 10 minutes at temperature. Heating and cooling were performed in pure hydrogen ambients. After different TiC samples were carburized under three different ethylene concentrations, it was discovered that no graphite formed on the TiC exposed to 0.1 and 0.2 % ethylene, while graphite was deposited on the TiC surface exposed to 0.5% ethylene. Therefore, the 0.2% C_2H_4/H_2 mixture was used for all further carburizations at 1250°C. When such carburizations were used, the TiC surface supported the deposition of single phase β-SiC.

As mentioned in the previous section, experiments for carburization at 1400°C were much more thorough since it was found that the titanium carbide crystal was much more reactive at this temperature. All carburization and SiC growth experiments at 1400°C were performed using 95% TiC + 5% VC monocrystals. For this set of experiments, the sample was heated, to 1400°C for 30 minutes, and then cooled; all three steps were performed in the ethylene + hydrogen ambient. The experimental matrix for a 1400°C carburization is shown in Table 3.

Table 3. 1400°C Carburization Experimental Parameters.

C_2H_2 Percentage in H_2	Resulting Film Morphology	Phases Identified by Raman
Very Low	TiC surface heavily etched.	No Raman active phases.
Low	Formation of a scale-like phase which flaked off the surface of the TiC.	Amorphous phase with two, broad Raman peaks.
Low	Formation of a scale-like phase which flaked off the surface of the TiC.	Amorphous phase with two, broad Raman peaks.
Low	Formation of a scale-like phase which flaked off the surface of the TiC.	Amorphous phase with two, broad Raman peaks.
Low	Formation of a scale-like phase which flaked off the surface of the TiC.	Amorphous phase with Raman peak at 690 wavelengths.
Optimal	Dark TiC surface, flat and smooth.	Extremely weak graphite spectrum.
High	Black film bubbled up on the TiC substrate.	Strong Raman spectrum of graphite; the deposited film is graphite

As Table 3 indicates, the exposure of TiC to ethylene/hydrogen mixtures at 1400°C produced *four* distinct surface morphologies and compositions. At very low ethylene percentages, the TiC surface was heavily etched. The surface was rather rough and had no distinct Raman response. Although the stoichiometry of such a surface was not characterized, it is inferred that the surface was heavily depleted of carbon because of the preferential volatilization of carbon by the hydrogen (see Figure 2). Such a surface is unsuitable for β-SiC deposition because of its rough texture and poor lattice match to β-SiC (Figure 1). A Ti-rich surface probably would not support β-SiC deposition since the Ti from the substrate would probably getter carbon deposited from the source gas leaving behind a surface which was silicon rich.

As discussed in the next section, titanium has a higher thermochemical propensity for combining with carbon than silicon. When the ethylene content was raised to a higher percentage, a new phase was formed in the TiC surface which then flaked off upon cool-down as seen in the SEM of Figure 13. As can be seen in Figure 14, the Raman spectra contains two unusually broad peaks, at 420 and 690 cm^{-1}. Such broad Raman peaks are indicative of an amorphous atomic structure. Therefore, this flaked-off phase could be a high-temperature Ti-C-H phase which is still low in carbon concentration. This phase occurred when the hydrogen concentration was insufficiently low to completely etch away the TiC, while the ethylene concentration was insufficient to ensure carburization without the formation of this amorphous phase. Again, a substrate surface coated by the amorphous phase would be an inappropriate substrate for ß-SiC growth because of the physical flaking of the surface and the amorphous crystalline structure of the phase.

The use of optimal levels of ethylene and hydrogen produced the best surface for ß-SiC growth, namely, a carburized TiC surface free from the amorphous phase, free from surface etching, and free of graphite deposition. An SEM of the optimal surface is seen in Figure 15. This mixture ensured that the TiC surface at 1400°C was monocrystalline and near stoichiometry. The ethylene activity in the reactor was optimal to almost saturate the TiC surface, yet not deposit graphite.

The fourth result of carburization was observed at a high ethylene diluted in hydrogen. This flow rate produced a layer of graphite which formed a dome on the TiC surface. The graphite domed layer was easily identified by its distinctive Raman spectrum while the TiC surface beneath the graphite was unetched and did not include the flaky, amorphous phase.

4.2 Silicon Carbide Growth Runs

Silicon carbide growth runs were divided into two regimes. The first set of growth runs were performed at temperatures between 1250 and 1310°C using the susceptor illustrated in Figure 4b. The second set of growth runs was performed at 1400°C using the susceptor illustrated in Figure 4c.

It is important to point out that there was greater temperature variability in the runs using the susceptor of 4b because its peak temperature could only be obtained using the maximum output of the 10 kW rf generator. Therefore, the highest temperature of each run using the Figure 4b susceptor was always achieved at the beginning of the run. As the run progressed, silicon carbide powder would form on the susceptor and along

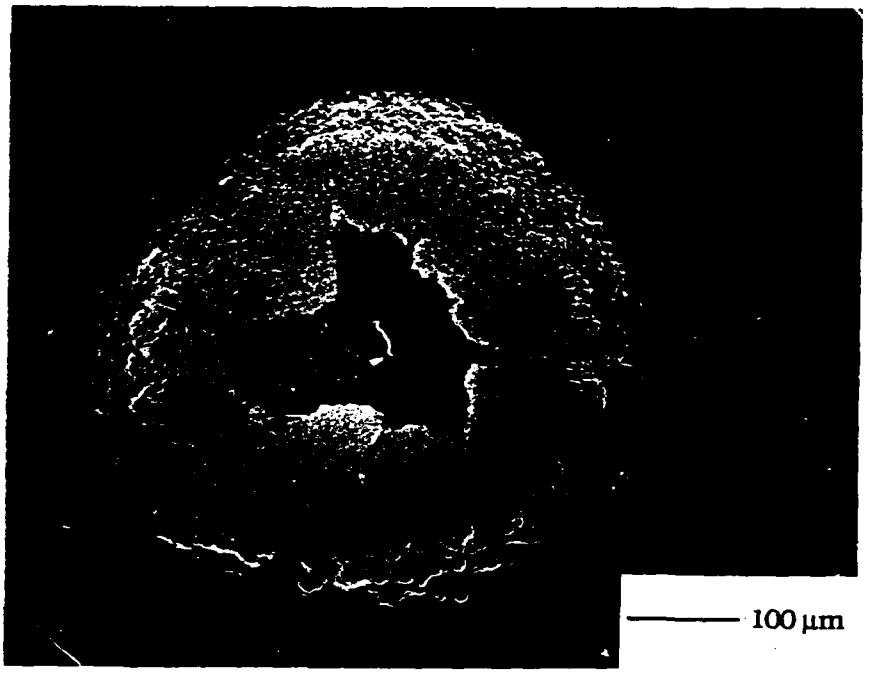

FIGURE 13. SEM MICROGRAPH OF AN AMORPHOUS PHASE CREATED DURING TiC CARBURIZATION AT 1400°C IN LOW PERCENTAGE ETHYLENE/HYDROGEN AMBIENTS.

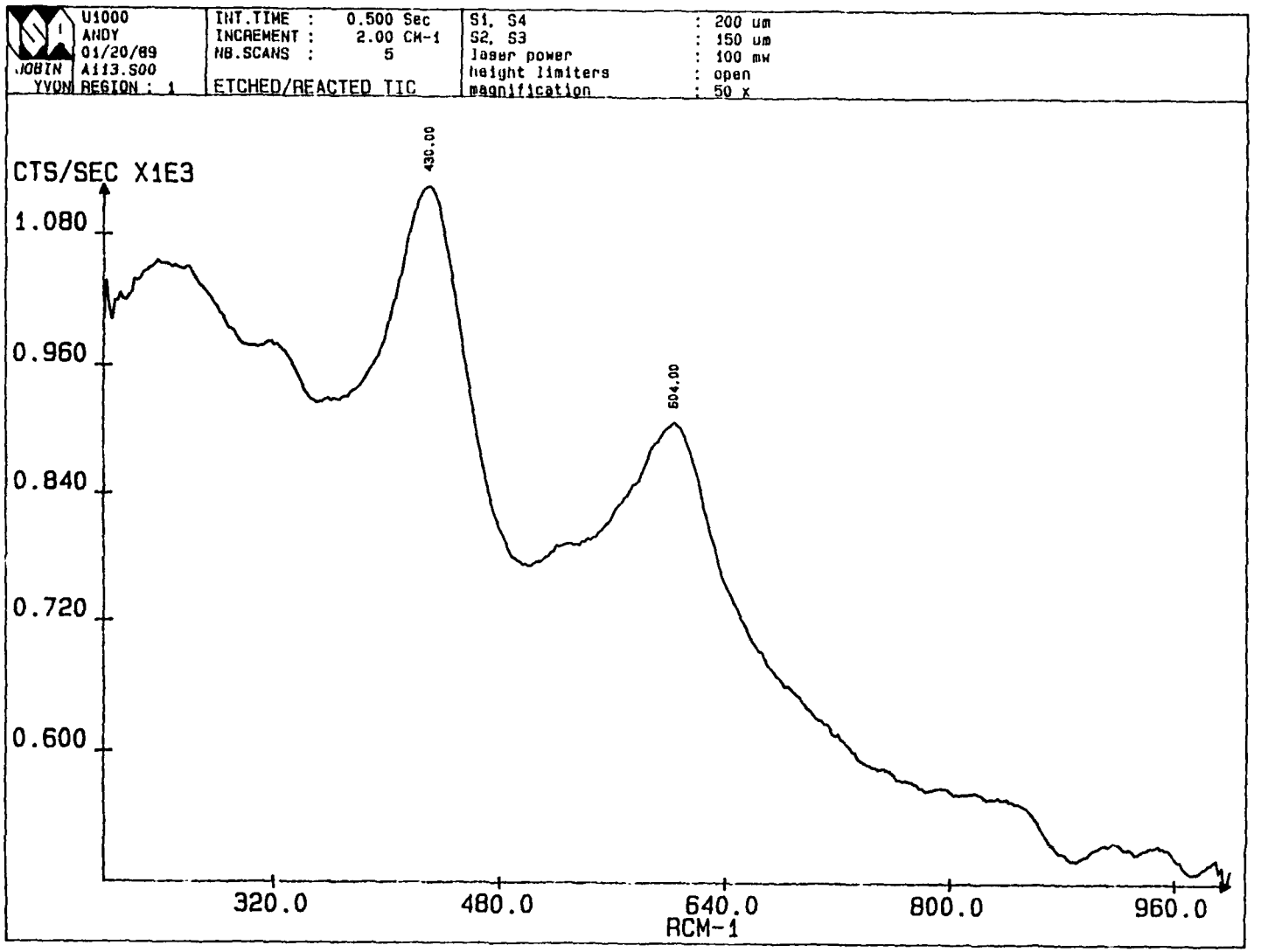

FIGURE 14. RAMAN SPECTRUM OF THE AMORPHOUS PHASE CREATED DURING TiC CARBURIZATION AT 1400°C IN LOW PERCENTAGE ETHYLENE / HYDROGEN AMBIENTS.

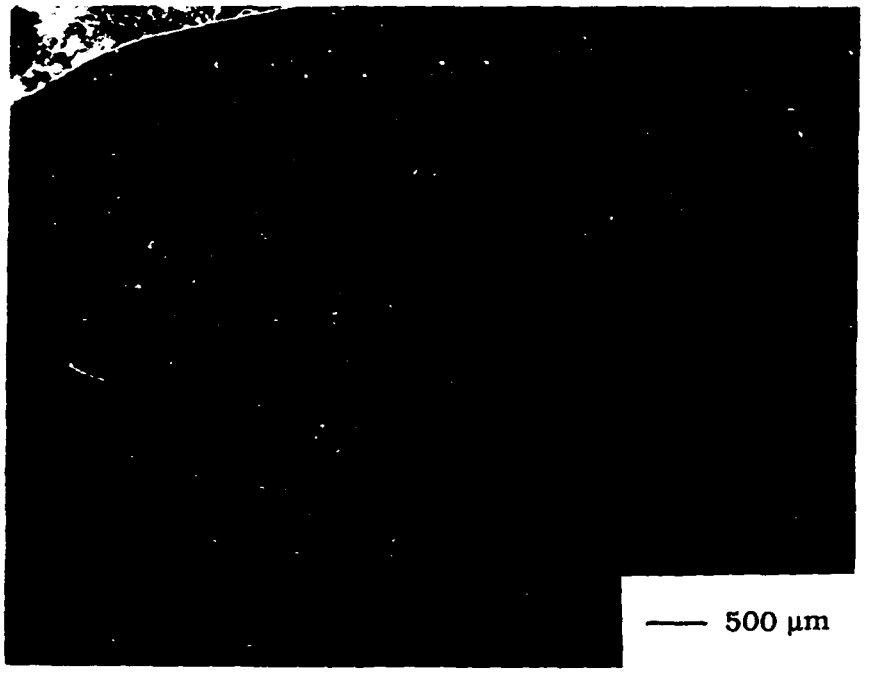

FIGURE 15. SEM MICROGRAPH OF FULLY CARBURIZED SUBSTRATE PRIOR TO β-SiC DEPOSITION AT 1400°C. Carburized in optimal Ethylene/Hydrogen Ambients at 1400°C.

the inside walls of the silica tube, steadily reducing the temperature. Runs were always terminated if the temperature dropped below 1200°C.

Use of the improved susceptor illustrated in Figure 4c permitted the initial attainment of 1400°C at only 70-75% rf generator output. As the run progressed, further deposition of silicon carbide powder and its cooling effect could be easily compensated by a steady increase in the rf generator output.

Consider first the deposition of β-SiC from mixtures of CH_3SiH_3, H_2, and Ar. Methylsilane growth runs were performed using the susceptors illustrated in Figure 4a and 4b. The cylinder of CH_3SiH_3 was empty before the susceptor of Figure 4c was created, therefore, CH_3SiH_3 was never used for growth runs at 1400°C. A film grown from 0.5 slm of Ar, 0.5 slm of H_2, and 0.5 sccm of CH_3SiH_3 at 700 torr and 1250°C was composed of only silicon.

When argon was used in conjunction with CH_3SiCl_3, it was observed that silicon was co-deposited with the β-SiC at 0.5 slm argon, 0.5 slm hydrogen and 0.5 slm MTS at 700 torr and 1250°C. Because the addition of argon was found to promote co-deposition of silicon regardless of whether methylsilane or MTS was used, further use of argon as a process gas was discontinued. The reasons for this were supported by thermodynamic arguments as discussed in Section 5.

The first use of MTS was performed using the susceptor with the pyrolytic boron nitride pedestal as illustrated in Figure 4a. As discussed in Section 5, a chemical reaction between the MTS and the pyrolytic boron nitride produced unacceptable powder formation on the susceptor and belljar walls. Because of the chemical reactivity between BN and CH_3SiCl_3, use of pyrolytic boron nitride pedestal was no longer used for any growth runs. All subsequent growth runs in the temperature range below 1300°C utilized the susceptor as illustrated in Figure 4b. Under these growth conditions it was discovered that single phase, polycrystalline β-SiC could be grown using MTS/hydrogen or methylsilane + ethylene/hydrogen mixtures.

It was observed that films deposited at 1250-1300°C from mixtures of CH_3SiH_3 and H_2 resulted in the co-deposition of silicon along with SiC. To inhibit silicon co-deposition, 0.2 sccm of C_2H_4 was flowed along with 1.5 sccm of CH_3SiH_3 diluted in 1. - 1.5 slm of H_2. The CH_3SiH_3 + C_2H_4 mixture was selected to attain a C/(C + Si) ratio of 0.4; the thermodynamic significance of this source gas ratio is discussed in Section 5. As predicted by thermodynamics, the CH_3SiH_3 + C_2H_4 mixture produced a film of single phase β-SiC, as demonstrated by the Raman spectrum of Figure 16. However, the film was polycrystalline.

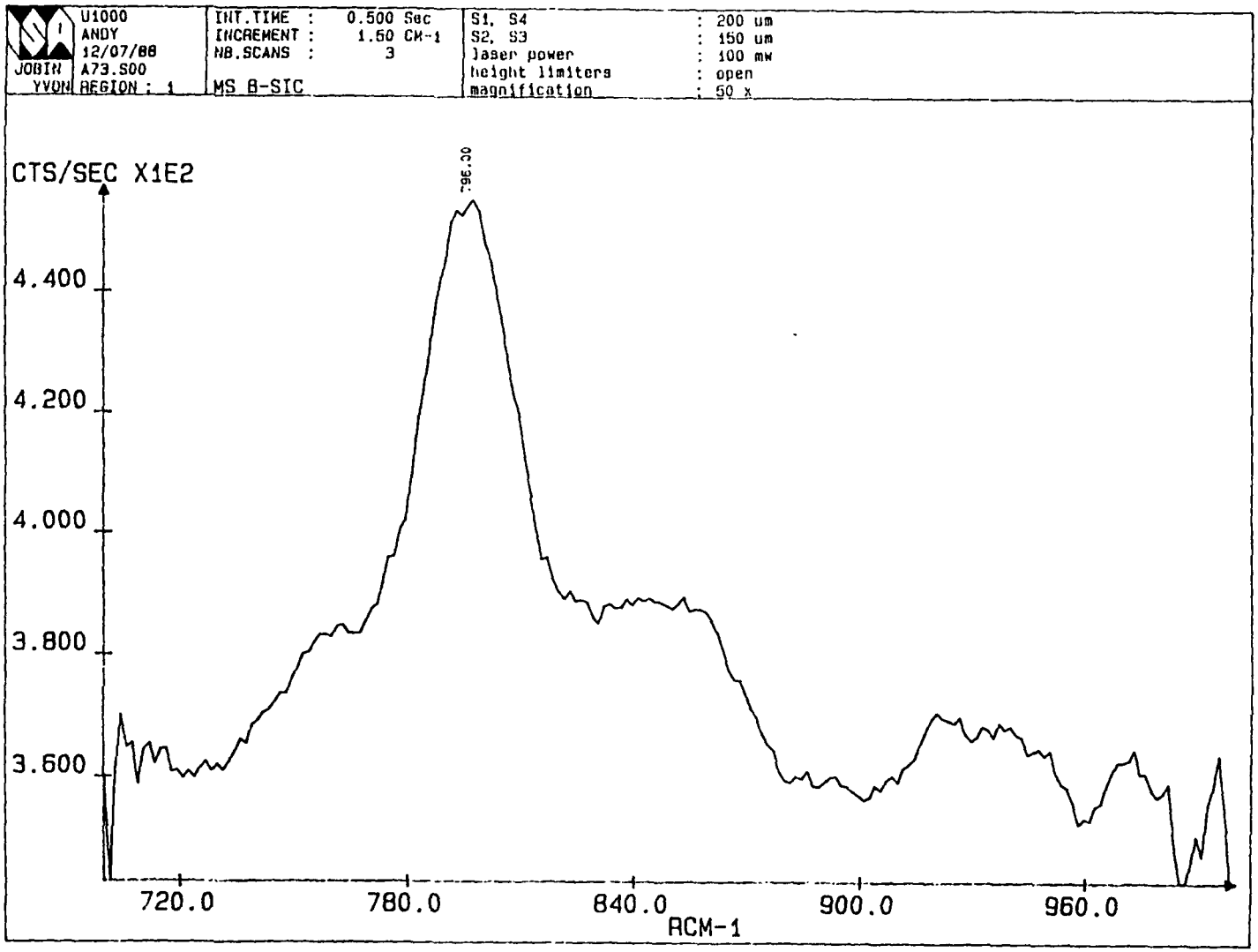

FIGURE 16. RAMAN SPECTRUM OF β-SiC FILM DEPOSITED AT 1250°C IN A METHYLSILANE/ HYDROGEN AMBIENT.

Single phase, polycrystalline ß-SiC could also be deposited from mixtures of CH_3SiCl_3 diluted in H_2. Again, single phase ß-SiC was observed as shown by its Raman spectrum of Figure 17.

After a series of experiments were performed in order to optimize the design of the susceptor illustrated in Figure 4c, the susceptor could easily sustain 1400°C. The improved susceptor was used to perform the high temperature carburization experiments described previously. After successful carburization of the TiC surface without (a) etching of the TiC, (b) formation of an amorphous surface phase, or (c) deposition of graphite.

Once the optimal carburization procedure was developed at 1400°C, DMI deposited a series of films from mixtures of MTS and H_2 immediately following carburization. When the percentage MTS fell below 2%, the TiC surface was severely etched. Depending on the percentage of MTS, the TiC could be transformed into the amorphous phase (Figures 13 and 14). At higher MTS percentages, a ß-SiC film would form, but the film would be severely uncut by severe etching of the TiC substrate. It was believed that the severe etching of the TiC at higher MTS percentages (e.g., 0.5 to 1%) was the result of HCl etching of the TiC. As reaction 2 indicates, for each mole of ß-SiC deposited, MTS releases 3 moles of HCl. HCl seems to etch TiC at 1400°C.

However, ß-SiC growth at 1400°C in 2% MTS for 10 minutes produced a film which probably contains a ≈ 1 µm layer of monocrystalline ß-SiC. The 10 minute run at 2% MTS produced a film of two distinct morphologies across its thickness. As shown in Figure 18, a cross-sectional SEM of a peeled-off area of the film, the first ≈ 1 µm is free of grain boundaries. The very smooth outer position of the film was in contact with the TiC substrate. Figure 19 is a Raman spectrum taken of the smooth surface of this sample. The Raman spectrum is predominantly ß-SiC, the weak α-SiC Raman lines are believed due to the thicker, polycrystalline portion of the film. Hence, DMI concludes the 2% MTS/H_2 run produced a heteroepitaxial, monocrystalline ß-SiC film which turned polycrystalline (with α-SiC contamination) after ≈ 1 µm of growth. The thick polycrystalline layer atop the thinner monocrystalline layer, probably cause the film to spontaneously flake off the TiC substrate during cool-down.

Attempts to repeat the 2% MTS run, but for a shorter time, were unsuccessful because DMI ran out of MTS source gas.

DMI believes that there is a connection between a relatively high % of MTS and successful heteroepitaxial growth of ß-SiC. Since growth rate is proportional to % MTS, a high, initial growth rate may be necessary to rapidly encapsulate and protect

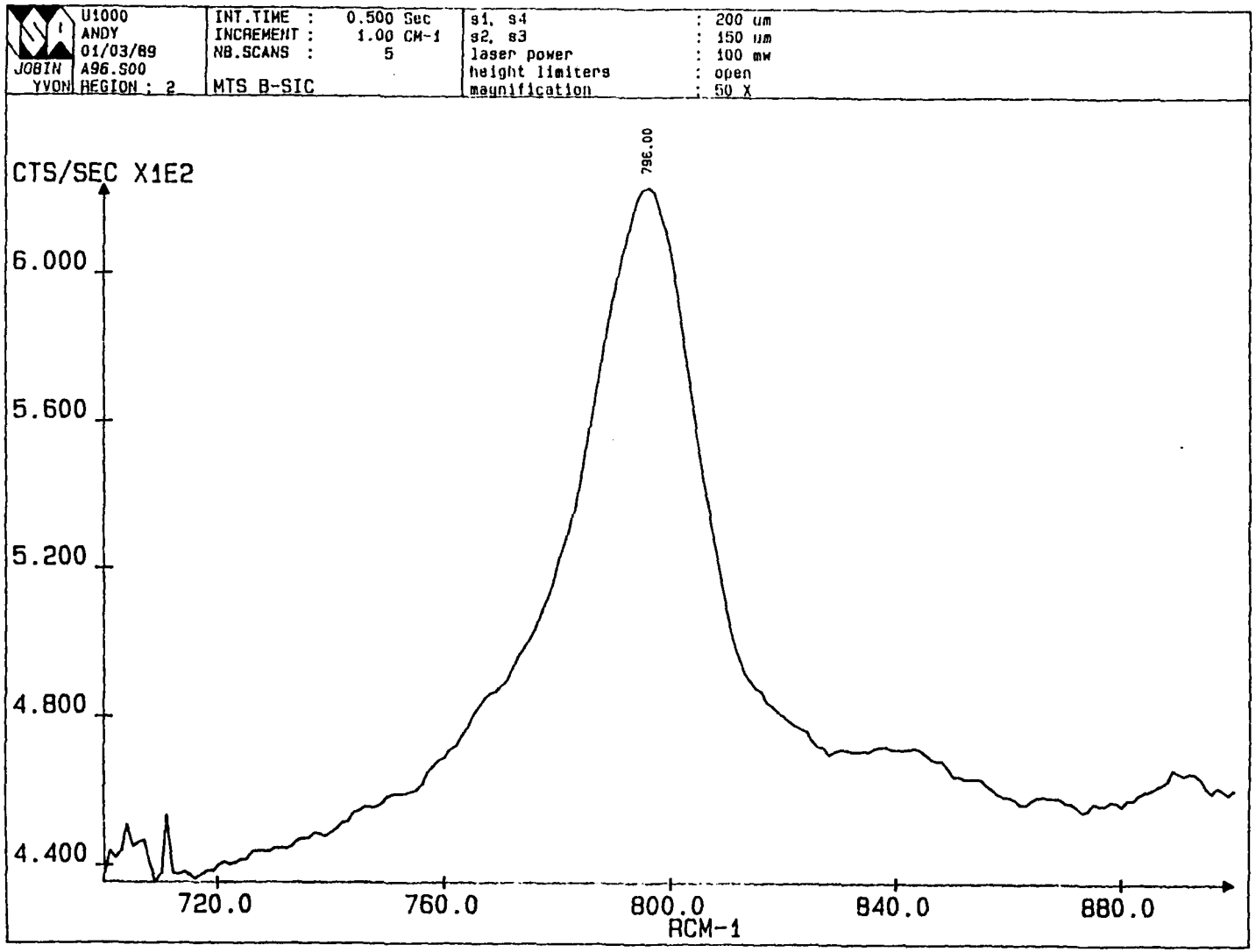

FIGURE 17. RAMAN SPECTRUM OF ß-SiC FILM DEPOSITED AT 1250°C IN AN MTS/HYDROGEN AMBIENT.

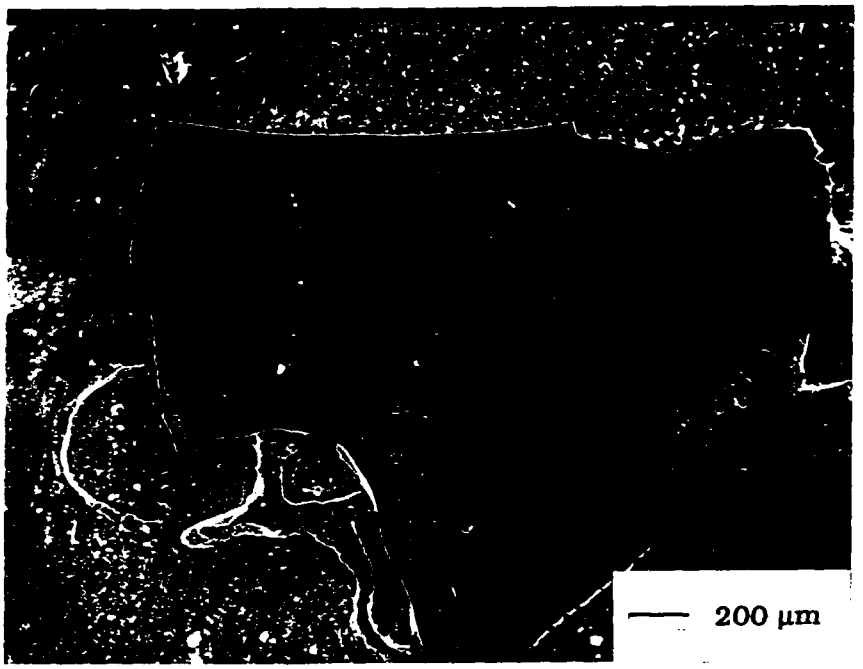

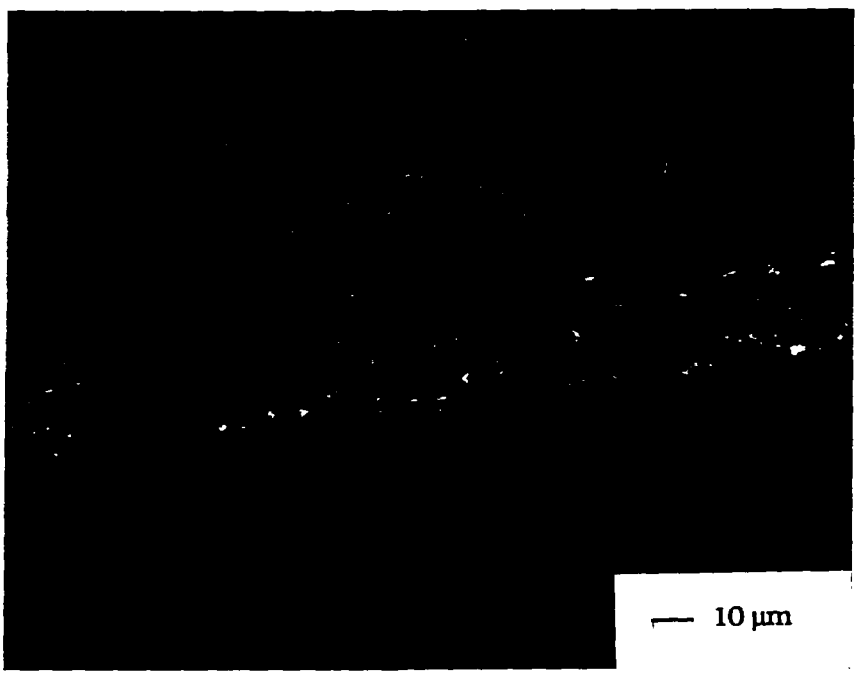

FIGURE 18. SEM MICROGRAPHS OF β-SiC FILM DEPOSITED AT 1400°C IN 2.0% MTS/HYDROGEN AMBIENT.

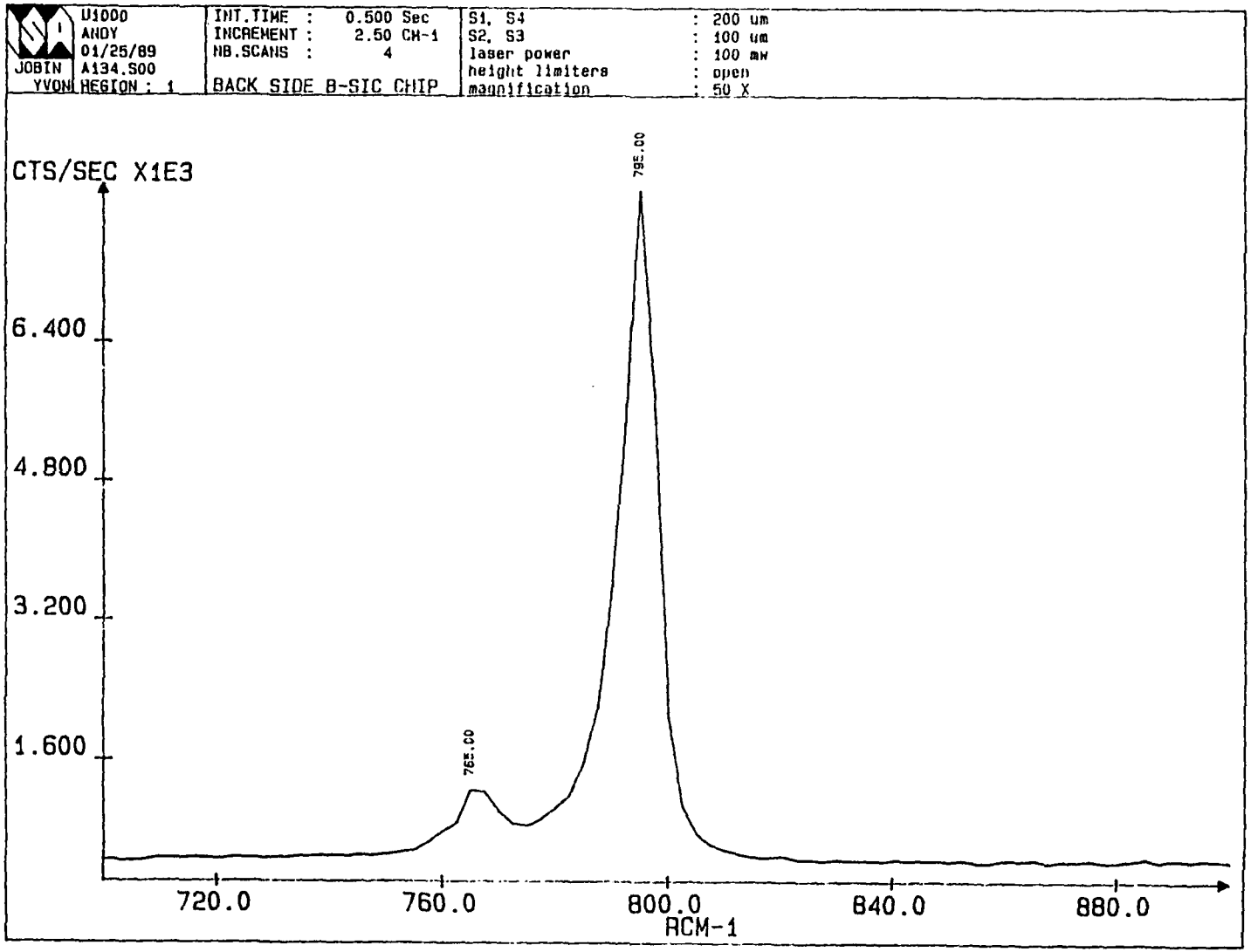

FIGURE 19. RAMAN SPECTRUM OF β-SiC FILM DEPOSITED AT 1400°C IN A 2.0% MTS/HYDROGEN AMBIENT.

the TiC substrate from subsequent HCl and/or H°, H_2 etching. The TiC_x substrate beneath the 2% MTS/film was smooth and free of any evidence of etching.

5. DISCUSSION

5.1 Thermodynamic Analysis of β-SiC Chemical Vapor Deposition

The chemical vapor deposition of monocrystalline β-SiC is most frequently performed in cold wall CVD reactors [11]. It has been shown that CVD of silicon carbide at temperatures below 1600°C is limited by the chemical reaction of the reactant gases at the substrate surface. It has been shown that CVD conditions similar to those used in this investigation are close to thermodynamic equilibrium [8]. Therefore, thermochemical calculations provide valuable guidance as to the selection of processing conditions.

Two excellent articles have been published describing the thermochemical analysis of SiC CVD. The first paper was published by A. I. Kingon, L. J. Lutz, P. Liaw and R. F. Davis of North Carolina State University [8]. The authors of that paper obtained an upgraded version of the computer program SOLGASMIX-PV from Prof. Karl Spear of Penn State University (Prof. Spear is a consultant to DMI). SOLGASMIX-PV uses linear programming to calculate the collection of chemical reaction products which would minimize the Gibbs free energy of a system, based upon the composition of the input gas mixture. SOLGASMIX-PV can predict the identity and relative amounts of various condensed and vapor species at thermodynamic equilibrium [12,13]. Kingon, et al. used SOLGASMIX-PV to generate a series of CVD phase diagrams. CVD phase diagrams are a map of equilibrium, condensed phase fields as a function of the input gas composition. Kingon, et al. examined the Si-C-H system as well as selected examples from the Si-C-H-Cl system.

A second paper on thermochemical analysis of silicon carbide deposition was by Fischman and Petuskey of the University of Illinois [9]. Fischman and Petuskey obtained upgraded SOLGASMIX-PV from Prof. Davis of NCSU. Fischman and Petuskey restricted their discussion to the Si-C-H-Cl system in which the Cl/Si molar ratio was fixed at 3; this is applicable to methyl trichlorosilane. Both papers emphasized that creation of single phase β-SiC is a sensitive function of temperature, total pressure and source gas composition. During this research effort, DMI found that the CVD phase diagrams published in these two papers were usually accurate, corresponding well to empirical determinations of deposited phases made by Raman spectroscopy.

5.1.1 CVD of SiC from the Si-C-H System

This three component system was examined by Kingon, et al. Their generic source gas mixture was silane, methane, hydrogen, and argon. The addition of argon was thermodynamically equivalent to the absence of hydrogen as a carrier gas. Although SOLGASMIX-PV was used to create various diagrams based on methane, silane and hydrogen, they performed calculations using other source gas mixtures such as silane, ethylene, and hydrogen. However, they discovered that final collection of condensed phases was approximately independent of the molecular form of the input gases; the important variable was the relative number of moles of Si, C, and H. Hence, by treating 1 mole of ethylene as equal to 2 moles of methane, the $SiH_4/CH_4/H_2$ CVD phase diagram was applicable to the use of ethylene. Methylsilane (CH_3SiH_3) was equivalent to 1:1 SiH_4/CH_4 if the H_2 dilution is at least 50:1.

Figure 20 is a series of CVD phase diagrams at atmospheric pressure or 10^5 Pa. It is immediately evident that use of argon as a carrier gas increases the probability of silicon or graphite co-deposition. Instead, ß-SiC formation is enhanced when the H_2/source gas ratio is at least 50. The authors note that the Si/(Si+C) ratio in the input gas should be approximately 0.4 to maximize deposition efficiency and minimize co-deposition of silicon or graphite. Because a 1:1 mixture of silicon and carbon is on the border line with co-deposition of elemental silicon, a small concentration of ethylene was flowed along with methylsilane in order to insure an overall silicon/silicon + carbon ratio of about 0.4. As was demonstrated, this procedure was effective in eliminating co-deposition of silicon.

Figure 20 is relevant to the vast majority of ß-SiC CVD research since most procedures occur at one atmosphere pressure. Jim Parsons [6] reported that ß-SiC deposition was optimized when he used 5 sccm SiH_4, 0.2 sccm C_2H_4, 2 slpm Ar and 0.9 slpm H_4 at 1400°C (1673 K) at 10^5 Pa. Parsons' growth conditions are equivalent to 5 sccm SiH_4, 0.4 sccm CH_4 and 900 sccm H_2. Therefore, his ratio $H_2/(SiH_4+CH_4)$ = 167 and his Si/(Si + C) ratio is 0.93. Thermodynamically, Parsons' conditions place his results clearly within the ß-SiC + Si phase field. Initial efforts by DMI to duplicate his work resulted in co-deposition of silicon. Co-deposition of silicon was prevented by using only hydrogen as the diluent gas and by slight additions of ethylene to the methylsilane.

As mentioned previously, DMI verified the observation made by So and Chun [14] that powder formation of silicon carbide on the walls of the reaction chamber is

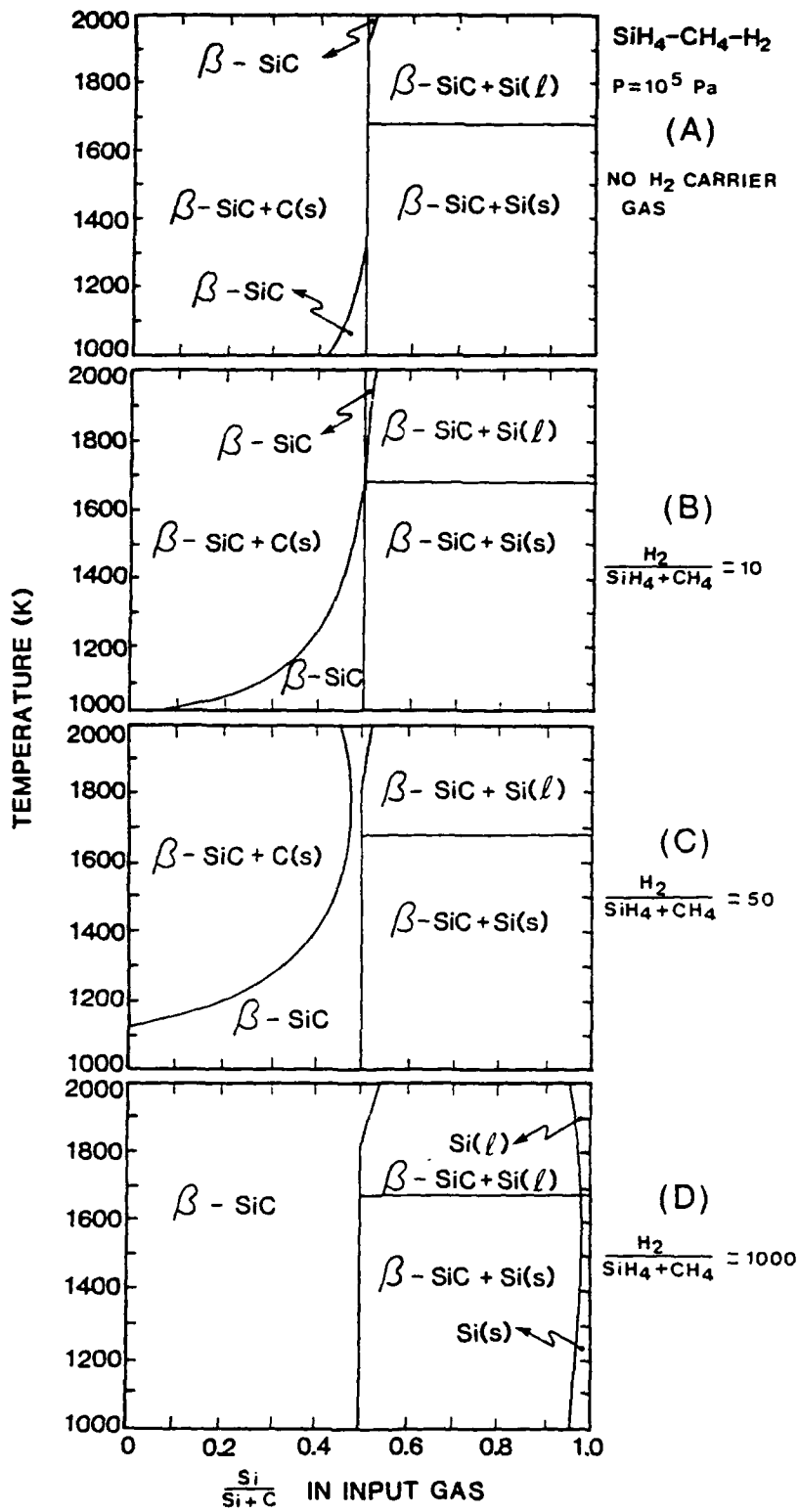

FIGURE 20. THE SYSTEM $SiH_4/CH_4/H_2$ AT 10^5 Pa TOTAL PRESSURE AND H_2 CARRIER GAS CONCENTRATIONS INDICATED. (Reproduced from Reference 8).

minimized at lower total pressures. Lower total operating pressure also increased substrate temperature at constant rf power due to a reduction of convective heat loss. DMI operated at a total pressure of 250 torr (3.3×10^4 Pa). CVD phase diagrams at 10^4 Pa are shown in Figure 21. The reduced total pressure decreases the size of the ß-SiC single phase field. However, if the Si/(Si + C) ratio is kept between 0.4 and 0.5, co-deposition of graphite is avoided. When the mixture of 1.5 sccm methylsilane + 0.1 sccm ethylene + 1.5 slpm of hydrogen at ≈ 1400 K, only single phase ß-SiC was deposited.

5.1.2 CVD of SiC from the Si-C-Cl-H System

This thermodynamic system describes deposition of silicon carbide from methyl trichlorosilane (CH_3SiCl_3) + H_2 mixtures. Kingon, et al. generated the CVD phase diagrams which appear in Figure 22 for the system MTS/hydrogen at three different total pressures. The figure indicates that use of MTS/hydrogen to form ß-SiC is less problematic than the use of methylsilane since there is no need to add a hydrocarbon to the MTS to prevent co-deposition of silicon. At either 10^5 or 10^4 Pa total pressure, it is thermodynamically necessary only to have a H_2/MTS ratio of at least 100.

Figure 23 is taken from the paper by Fischman and Petuskey [9] and considers the case where the Cl/Si molar ratio is fixed at 3, but C/Si ratio is variable. The four graphs in Figure 23 at log(C/Si) = 0 correspond with the graphs of Figure 22. Figure 23 indicates that in the presence of Cl/Si = 3, the one-to-one carbon-to-silicon stoichiometry which is automatically present in MTS is optimal in ensuring deposition of single phase ß-SiC. Therefore, the addition of almost any amount of hydrocarbon to MTS would almost certainly produce co-deposition of graphite.

Figure 24 is a CVD phase field for the situation at 1600 K (1323°C), 10^5 Pa, and C/Si = 1. This figure illustrates the relative roles of chlorine and hydrogen on the thermodynamics of silicon carbide CVD. Hydrogen removes carbon from the condensed phase, while addition of chlorine removes silicon. Figure 24 also indicates that a large dilution of hydrogen is necessary in order to prevent co-deposition of graphite while a lower chlorine content prevents co-deposition of silicon.

At ICACSC '88, Nishino and Saraie [15] reported the growth of ß-SiC from mixtures of 0.1 sccm Si_2H_6, 0.1 sccm C_2H_2 and 1 sccm HCl and 1 slpm H_2 at 1300°C. The addition of HCl reduced the growth rate of ß-SiC, but permitted them to grow single phase ß-SiC at temperatures down to 1150°C. Nishino and Saraie used a Cl/Si ratio of

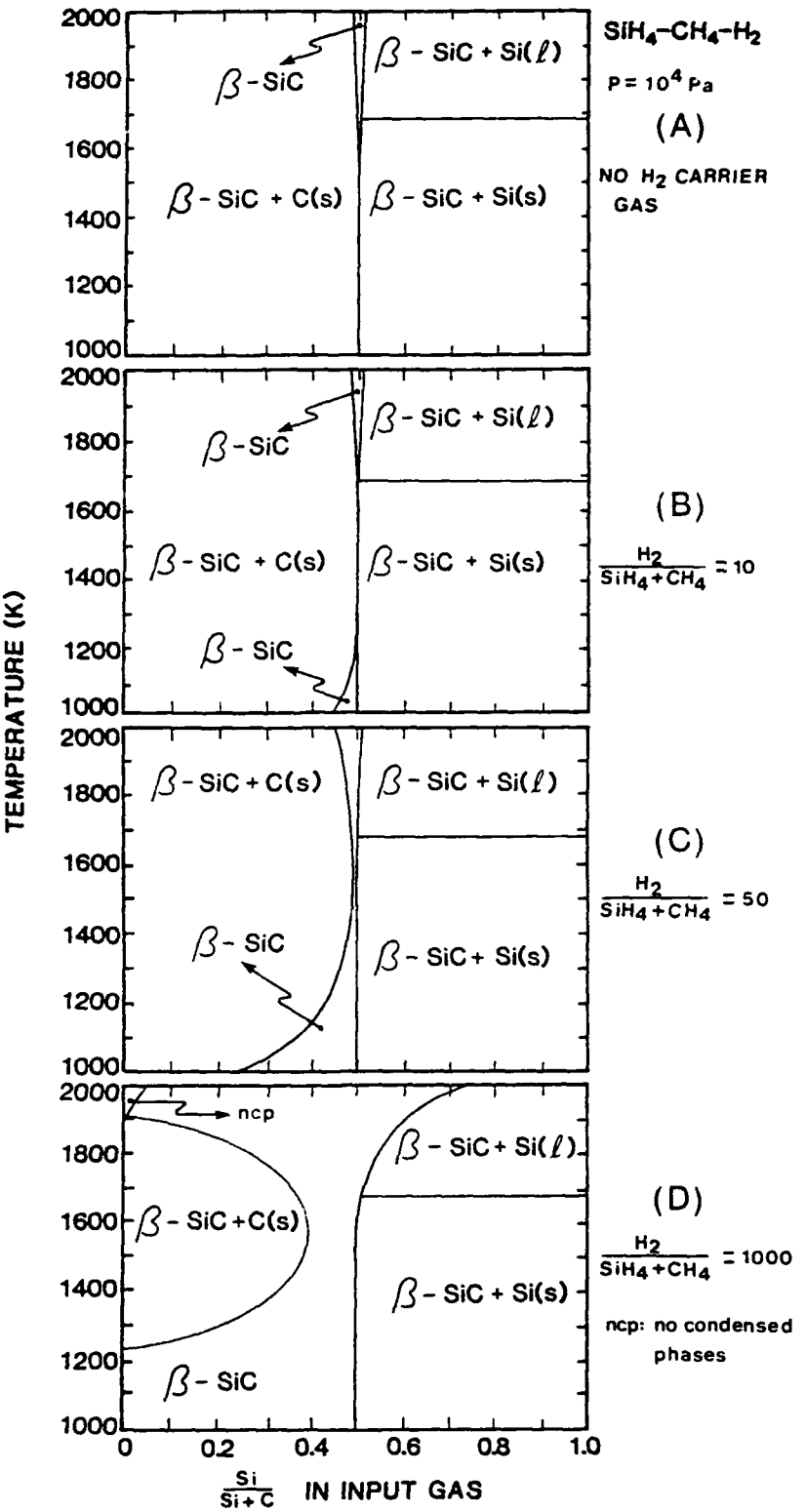

FIGURE 21. THE SYSTEM $SiH_4/CH_4/H_2$ AT 10^4 Pa TOTAL PRESSURE AND H_2 CARRIER GAS CONCENTRATIONS INDICATED. (Reproduced from Reference 8).

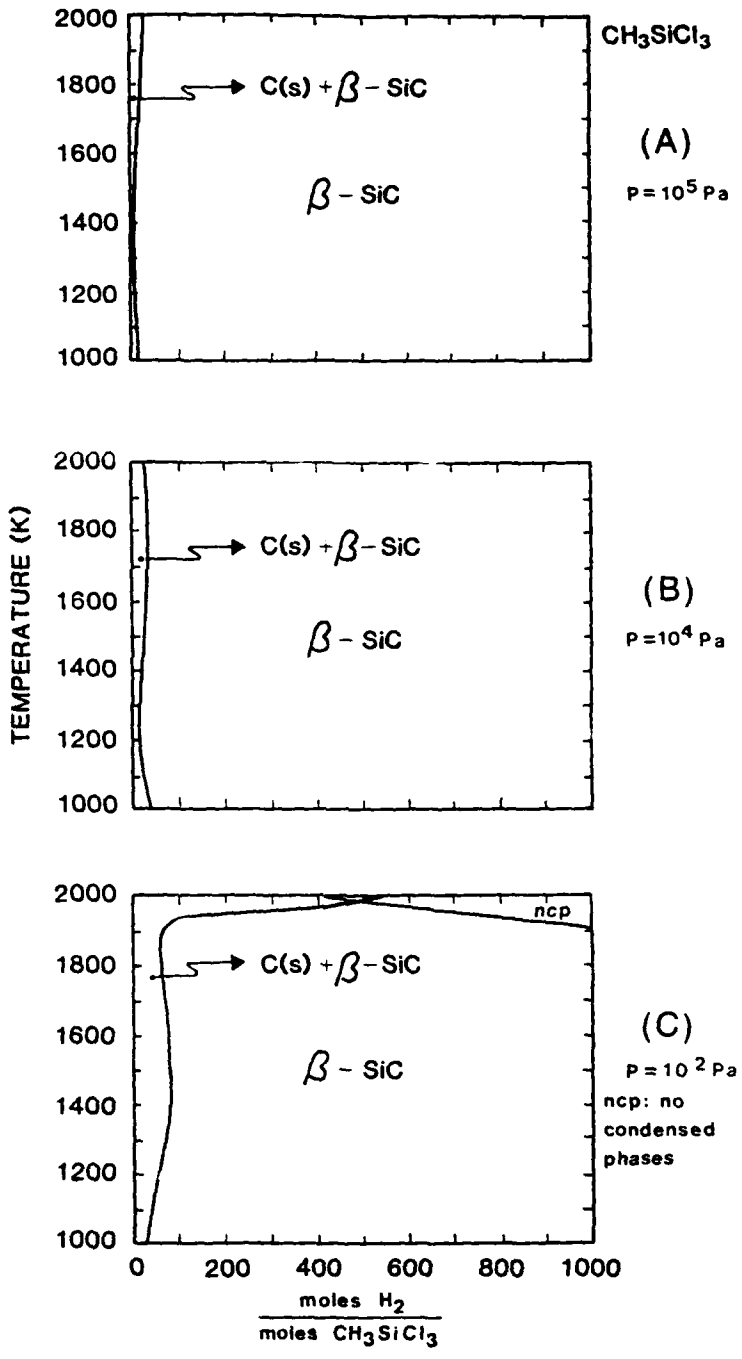

FIGURE 22. THE SYSTEM CH_3SiCl_3/H_2 AT THE TOTAL PRESSURES INDICATED. (Reproduced from Reference 8).

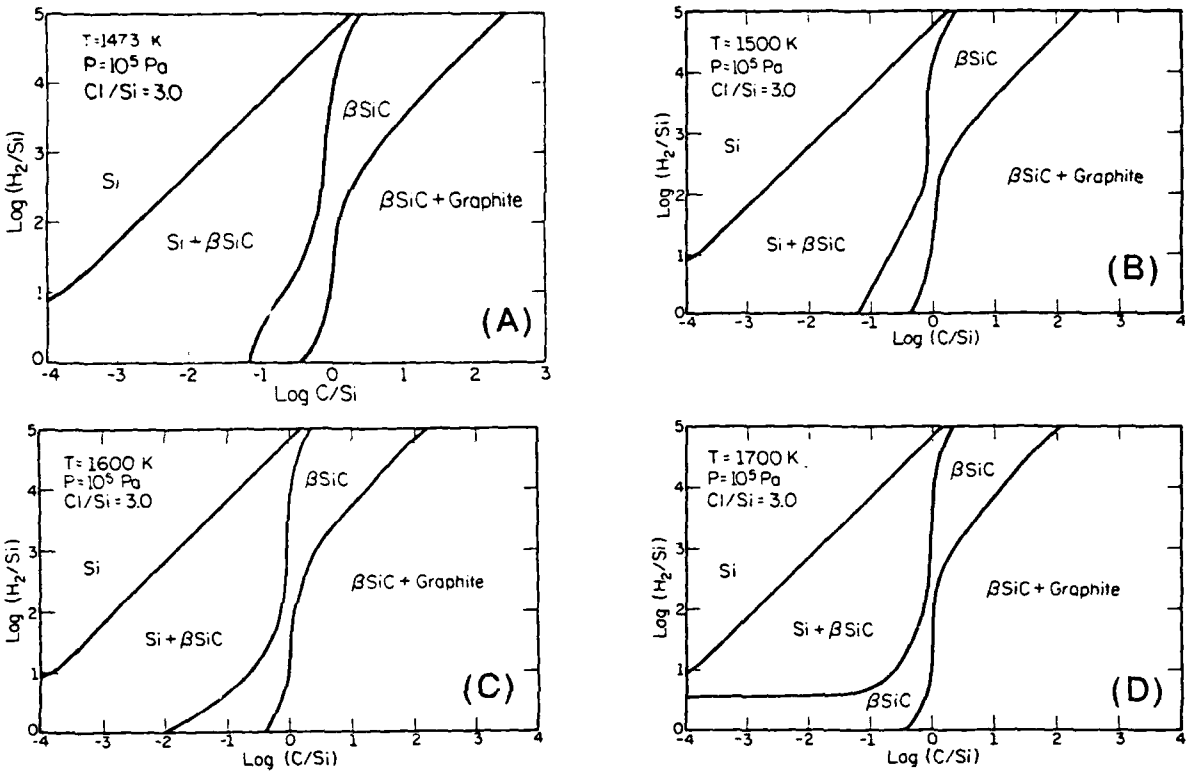

FIGURE 23. STABILITY DIAGRAMS OF CONDENSED PHASES IN EQUILIBRIUM WITH A GAS PHASE IN THE SYSTEM Si-C-Cl-H AS A FUNCTION OF H_2/Si AND C/Si RATIOS FOR Cl/Si = 3 AT (A) 1473K, (B) 1500K, (C) 1600K and (D) 1700K. Elemental ratios represent composition of entire system which is also initial gas reactant composition in CVD processes. (Reproduced from Reference 9).

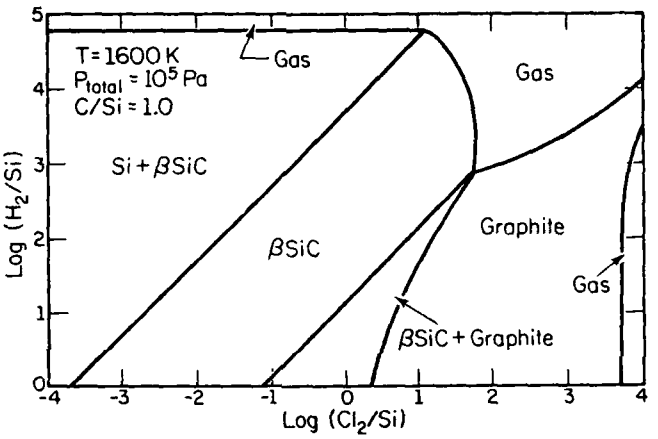

FIGURE 24. STABILITY DIAGRAM OF CONDENSED PHASES IN EQUILIBRIUM WITH A GAS PHASE IN THE SYSTEM Si-C-Cl-H AS A FUNCTION OF H_2/Si AND Cl_2/Si RATIOS FOR CONSTANT C/Si = 1. Elemental ratios represent composition of the entire system which is also composition of initial gas reactants. (Reproduced from Reference 9).

5. Therefore, their addition of HCl to mixtures of Si_2H_6 and C_2H_2 resulted in a thermodynamic situation similar to the use of CH_3SiCl_3 and hydrogen. However, as pointed out by Parsons, the use of MTS was preferred because it requires the use of only 2 mass flow controllers instead of the 4 mass flow controllers employed by Nishino and Saraie.

Figure 25 demonstrates the efficacy of methyl trichlorosilane as a single point source of silicon carbide. MTS is the ideal single point source for β-SiC since Cl/Si = 3 and C/Si = 1. This figure also indicates that slight deviations off C/Si = 1 stoichiometry would result in co-deposition of silicon or graphite.

5.1.3 Future Use of Thermochemical Models

The published thermodynamic analyses of Kingon, et al. [8] and Fischman, et al. [9] on the chemical vapor deposition of SiC proved to be extremely valuable during DMI's research. Based on this small amounts of ethylene to methylsilane to ensure a ratio of carbon to silicon of 0.4. The published CVD phase diagrams provided valuable guidance in selecting source gas mixtures when the total pressure was reduced from atmospheric pressure to 250 torr. Figure 24 assisted in the determination of the ethylene/methylsilane ratio needed to prevent co-deposition of silicon.

As mentioned previously, the person who taught Kingon and co-workers at North Carolina State University how to use SOLGASMIX-PV was Prof. Karl Spear of Penn State University. Prof. Spear is a co-founder of DMI and is a consultant to the Company. During this Phase I research, DMI found the SOLGASMIX-PV analyses published by others to be invaluable. Therefore, during the Phase II program, DMI will propose the utilization of its own SOLGASMIX-PV software to better design its CVD processes. SOLGASMIX-PV will be used to help select dopant gases for β-SiC. SOLGASMIX-PV will permit computer modeling of hypothetical CVD reactions in order to eliminate problematic β-SiC chemical vapor deposition parameters. For example, it has been mentioned that trimethyl aluminum (TMA) is not satisfactory as a dopant for β-SiC during heteroepitaxial growth because TMA has a low decomposition temperature [10]. SOLGASMIX-PV can be used to evaluate alternative sources for *in situ* aluminum doping at growth temperatures around 1400°C.

SOLGASMIX-PV can also be used to test the chemical compatibility of various susceptor/platen materials with the source gases at the various temperatures. If DMI had been operating SOLGASMIX-PV during the Phase I program, SOLGASMIX-PV would have been used to test the chemical compatibility of pyrolytic BN with CH_3SiCl_3.

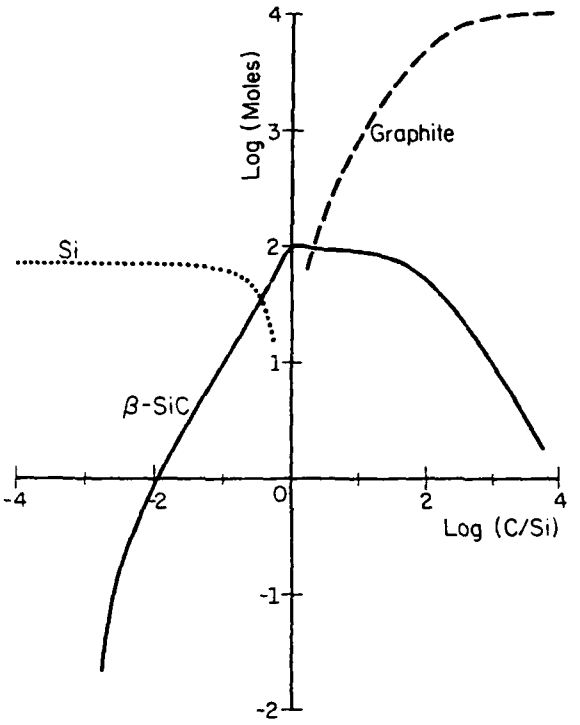

FIGURE 25. PROPORTIONS OF CONDENSED PHASES IN MOST STABLE SITUATION FOR T = 1600K, H_2/Si= 100, AND Cl/Si = 3 AS A FUNCTION OF C/Si RATIO. This diagram indicates that CH_3SiCl_3 is an excellent single point source for β-SiC. (Reproduced from Reference 9).

Since SOLGASMIX-PV would have predicted the formation of NH_4Cl, BN would not have been used in contact with MTS.

5.2 Film Morphology

The results of this research agree with other published research on the physical structure of CVD deposited silicon carbide films. Rough, polycrystalline films were always deposited at temperatures below 1300°C regardless of gas phase composition. Figure 26 is a diagram published by Chin, Gantzel and Hudson [16] which illustrates SiC film morphology as a function of hydrogen dilution, total pressure and temperature. Chin, et al. grew SiC films from mixtures of methyl trichlorosilane and hydrogen. The figure correlates reasonably well to recent observations over the growth conditions used in this study. Since Chin, Gantzel, and Hudson did not use suitable, monocrystalline substrates (such as TiC), they never attained heteroepitaxial, monocrystalline ß-SiC films. (Interestingly, the paper never mentions their substrates; it is guessed that they used graphite). However, epitaxial growth requires conditions of thermodynamic stability plus high surface atom mobility; under such conditions, a polycrystalline film is highly angular. As noted in Figure 26, Chin, et al. found that deposition of angular or faceted morphology was enhanced at low deposition pressures, high hydrogen dilutions, high hydrogen/MTS ratios, and high substrate temperatures.

Kong, et. al. [17] grew ß-SiC on 6H alpha silicon carbide substrates at 1410°C. Kong, et al. used a fixed source gas mixture of $SiH_4/C_2H_4 = 2$ and varied the amount of hydrogen diluent. They noted that in their barrel reactor, the morphology of the film changed dramatically as a function of dilution. Under identical conditions of temperature and total flow rate, the morphology of the film was rough and granular at a source gas/hydrogen ratio of 3/3000 while the morphology became flat and epitaxial at a source gas/hydrogen ratio of 1/3000.

DMI observed, as did other researchers, that single phase ß-SiC can be deposited with a wide range of morphologies and that the morphology is heavily controlled by the details of the deposition parameters. Relative flow rates and reactant gases and hydrogen, temperature and total pressure play an important role thermodynamically and kinetically. However it is also important to point out that the absolute gas flow in the reactor also plays an important role. Nishino et al. [18] emphasized that the flow rate and flow pattern of the MTS in their CVD reactor were absolutely critical. When

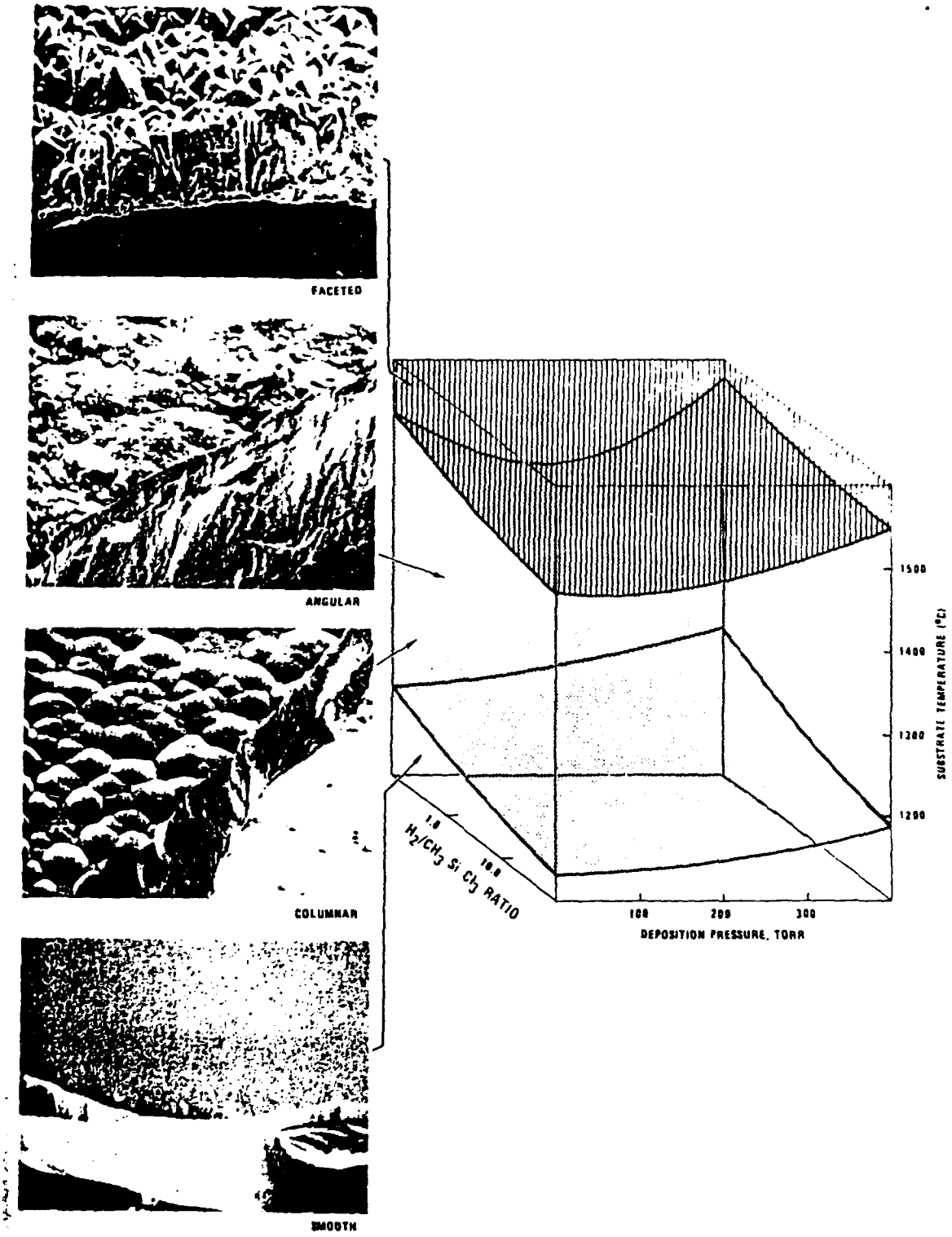

FIGURE 26. MORPHOLOGY OF POLYCRYSTALLINE SiC FILMS AS A FUNCTION OF H_2/CH_3SiCl_3 RATIO, TEMPERATURE AND PRESSURE. Angular or faceted films are indicative of a high surface atom mobility. (Reproduced from Reference 16).

they grew β-SiC at 1300°C in a horizontal tube CVD reactor, film morphology was only satisfactory when the MTS flow rate was at or below 1 sccm.

Nishino, et al. also found that the cross-sectional shape of the silica reactor tube affected the thickness uniformity of their heteroepitaxial β-SiC films on Si. Uniformity of his films improved when the cross-section of the silica tube was square rather than circular. In DMI's system, the area of the susceptor was only 13% the inner cross-sectional area of the reaction chamber. Gases were injected from a stainless steel tube (≈ 6 mm diameter) whose orifice was 17 cm away from the substrate surface. Because of time limitations, DMI did not experiment with varying the distance between the inlet orifice and the substrate surface. Examination of improved reactor geometries and flow rate patterns will be the subject in Phase II.

5.3 TiC as a Substrate for Heteroepitaxial Growth of β-SiC

Research by Parsons, Bunshah, and Stafsudd [1] and by Parsons and co-workers [6,10] has clearly demonstrated that semiconductor grade β-SiC can be heteroepitaxially grown on monocrystalline TiC substrates. Heteroepitaxial growth of β-SiC onto TiC has been demonstrated by reactive evaporation and by chemical vapor deposition (CVD). If the TiC substrate is of good quality, the resulting β-SiC crystals have a very low density of stacking faults and other crystalline defects.

TiC is an excellent substrate for β-SiC for a number of reasons. TiC and β-SiC have similar lattice constants. At room temperature, the lattice constant of β-SiC is 4.36Å, while the lattice constant of TiC is 4.33Å at stoichiometry. TiC has a range of stoichiometries which control the lattice constant as shown in Figure 27 [6]. β-SiC and TiC have similar thermal expansion over a wide temperature range, as shown in Figure 28 [6,19]. TiC's slightly larger thermal expansion is fortuitous since it places the β-SiC film in slight compression upon cool-down after film growth. Generally, epitaxial films in slight compression usually exhibit smoother morphology than films in tension [10]. Ti is also electrically inert in β-SiC; indiffusion of Ti into β-SiC can be prevented by saturating the TiC surface with carbon immediately before β-SiC growth [6]. It has been discovered empirically that *any* TiC crystallographic orientation will support heteroepitaxy of β-SiC [10]. TiC is a good electrical conductor with a work function of ≈ 3 eV; TiC forms a good ohmic contact to n-type β-SiC [10].

Currently, the only viable, alternative substrate for heteroepitaxy of semiconductor grade β-SiC is monocrystalline 6H-SiC. Research into the synthesis of 6H SiC using the modified Lely process is actively being pursued by North Carolina

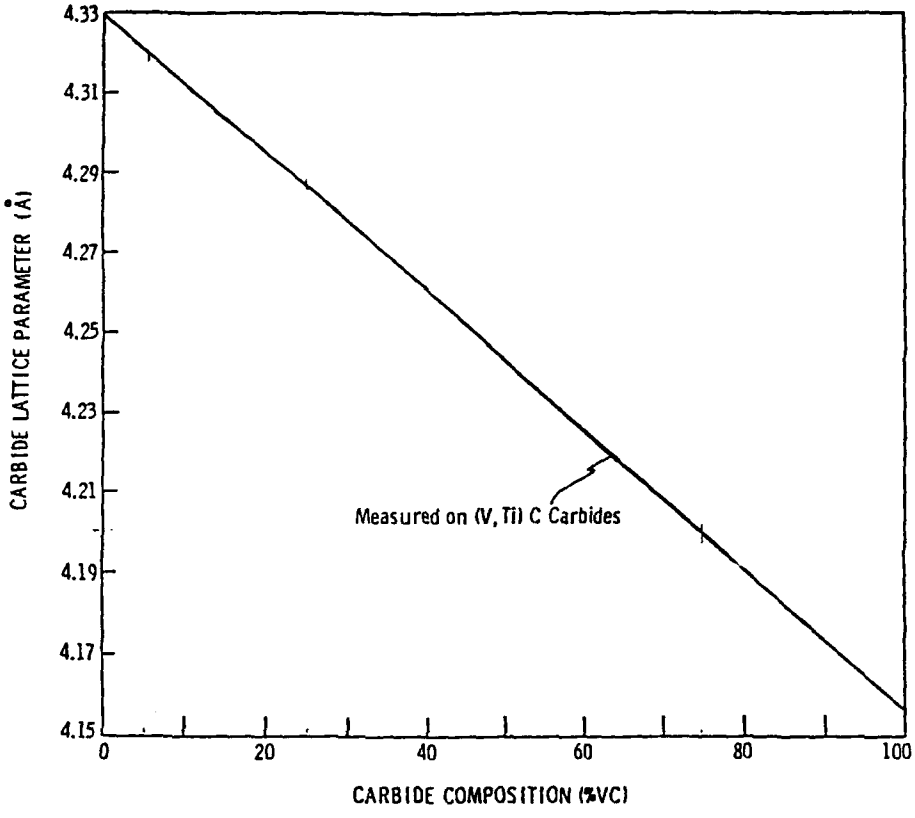

FIGURE 26. MEASURED LATTICE PARAMETER OF (Ti,V)C SOLID SOLUTION AS A FUNCTION OF MOLE PERCENT VC. (Reproduced from J. Green, J. Venables, R. Viswanadham and W. Precht, "Development of Cemented Alloy Carbides for Hard Rock Boring," Final Report to National Science Foundation Grant APR 74-21441, Martin Marietta Laboratories, (1977)).

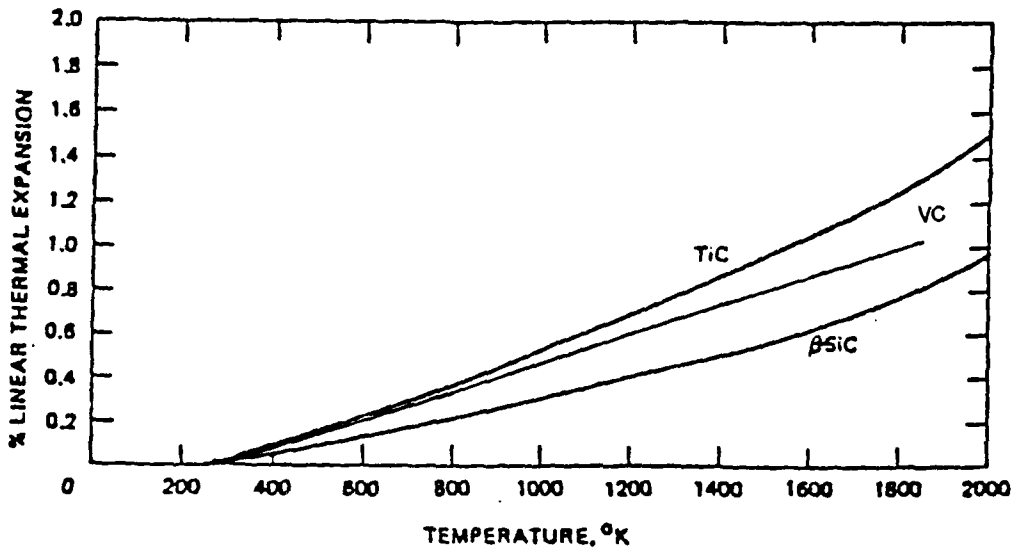

FIGURE 28. PERCENT LINEAR THERMAL EXPANSION OF TiC, VC and ß-SiC AS A FUNCTION OF TEMPERATURE. (Reproduced from Reference 6 with additional data from Reference 19).

State University, Cree Research and Seimens of Germany [20]. Cree Research has successfully grown 1" diameter monocrystals of 6H SiC. However, recent successes in 6H SiC crystal growth have prompted recent discoveries of the limitations of 6H SiC as a substrate for β-SiC. *Double positioning boundary defects* have been observed in β-SiC films grown on 6H substrates. Max Yoder of the Office of Naval Research [21] has explained this crystalline defect as follows:

> "In hexagonal material with the basal plane horizontal (i.e., the c-axis up) there are six atoms in the surface plane to which depositing atoms can nucleate. In the cubic material, there can be only three bonds attached to the six surface plane atoms. These nucleating cubic crystal forming atoms attached to every other atom of the hexagonal substrate. They have two possibilities of which group of three atoms to which they will attach. The next depositing/nucleating atoms may align in the same manner OR they may nucleate to surface atoms in a cubic unit cell which is rotated 60° from the initial depositing atoms. Thus, the atoms can position themselves in two ways, and this is called double positioning boundaries (between grains in the overlying cubic crystal)."

In contrast to α-SiC, TiC has rocksalt structure. Since TiC is cubic, it cannot generate double positioning boundary defects in the zincblende structure of β-SiC. Parsons et al. [10] recently reported that *any* crystallographic face of TiC supports β-SiC heteroepitaxy. This contrasts sharply with 6H SiC substrates in which even slight deviations from the (0001) surface results in epitaxial growth of α-SiC. Attempts to eliminate double positioning boundary defects by the use of slightly off-axis 6H SiC crystals has always resulted in the growth of α-SiC layers.

Another problem with large-area, 6H SiC crystals is their spatial nonuniformity in polytype. Parsons [6] mentioned that all large area 6H SiC monocrystals he has examined were, in fact, composed of various polytypes over their surface. Inhomogeneous polytypes may produce inhomogeneous β-SiC heteroepitaxial films. Therefore, TiC appears superior to 6H SiC as a substrate for the heteroepitaxial growth of β-SiC because TiC has: (a) rock salt structure, (b) exactly one polymorph and no polytypes, and (c) the ability to grow β-SiC on any crystalline face.

5.4 TiC Crystals and 95% TiC + 5% VC Crystals

At the start of this Phase I program, DMI obtained TiC monocrystals from its consultants R. Bunshah and C. Deshpandey of UCLA. These TiC crystals were rather small and had typical dimensions of 4 x 4 millimeters as shown in Figure 29. As discussed previously, these crystals contained pinholes and subgrain boundaries. The

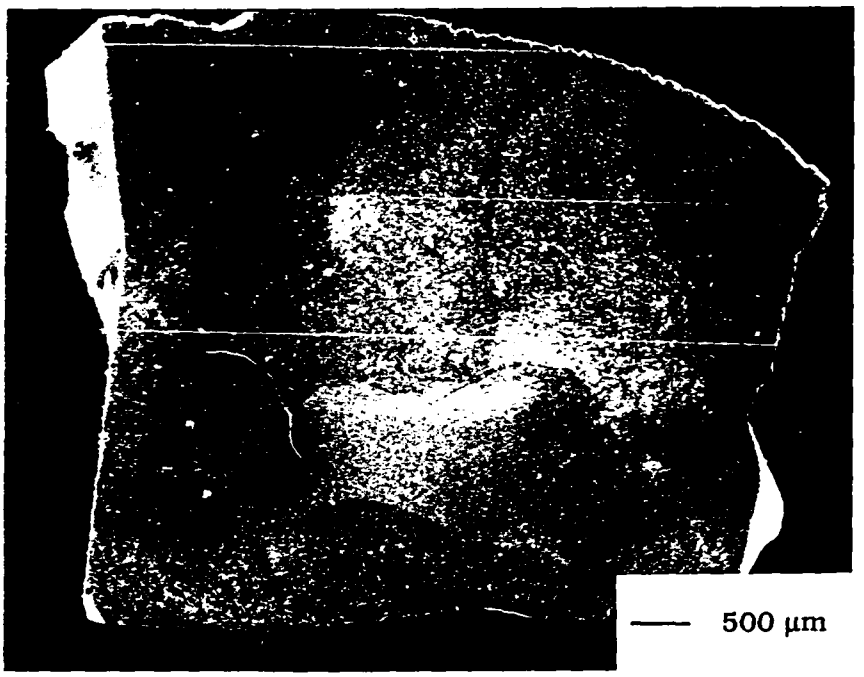

FIGURE 29. SEM MICROGRAPH OF SUBGRAIN BOUNDARIES EXISTING IN TiC SUBSTRATES RECEIVED FROM R. BUNSHAH.

subgrain boundaries in the TiC could be made clearly visible by patterns of β-SiC deposition. The subgrain boundaries resulted in highly dissimilar SiC depositions on either side, indicating a possible TiC substrate orientation effect for polycrystalline SiC films. TiC crystals used by DMI were made by the float zone process. This process is the only demonstrated method for growing monocrystalline ingots of TiC greater than 1 cm in diameter.

Parsons, et al. [10] recently enumerated the problems Hughes Research Laboratories is experiencing with the 2" diameter single crystals of TiC internally produced by Hughes. Hughes' TiC crystals are grown by float zone refining of hot-pressed TiC. Parsons, et al. noted two major problems with their TiC substrates. First, the TiC contained pinholes which produced pinholes in the β-SiC epi films, and second, the TiC contained subgrain boundaries which generated grain boundaries in the β-SiC film. Parsons noted that pinholes in TiC are primarily caused by transition metal oxide impurities in the starting material which precipitate during the float zone process and are eventually etched. Parsons also noted that pinholes in the TiC substrate create pinholes in the β-SiC epitaxial film. Parsons discussed formation of subgrain boundaries in the TiC ingots produced by Hughes. He noted that subgrain boundaries formed in the TiC ingot due to constitutional supercooling. Constitutional supercooling was the result of jerky motion of the stepper motors of the float zone apparatus, combined with impurities in the TiC. From the data presented in Section 4, it seems the original samples of TiC obtained from Dr. Bunshah contained many of the same crystalline defects described by Jim Parsons of Hughes.

During his talk at ICACSC '88, Parsons noted that the subgrain boundaries and pinholes of the TiC are *not* an intrinsic problem of TiC, but are an artifact of processing. To prove his assertion, he noted that superior TiC monocrystals have been fabricated outside of Hughes. He said the best TiC he had ever used as a substrate was grown by the float zone process by Mr. Walter Precht of Martin Marietta Laboratories in 1962. Parsons used Precht's TiC crystals for Parsons' dissertation research at UCLA. Precht's TiC was free of pinholes and subgrain boundaries and produced outstanding β-SiC heteroepitaxial films. Fifteen days after Parsons' remarks in Santa Clara, Richard Koba and Reznor Orr of DMI visited Walter Precht at Martin Marietta. Mr. Precht agreed to consult for DMI and assist in DMI's β-SiC effort.

Mr. Precht supplied DMI with a remnant of a 1 cm diameter boule of the alloy 95% TiC + 5% VC. Mr. Precht did not have available any pure single crystals of TiC. However, as Figure 27 indicates, 5% VC content does not significantly reduce the lattice constant of TiC. The lattice constant of the 95% + 5% VC crystal should be 4.32 Å as

opposed to 4.33 Å for 100% TiC. The alloy's a_0 = 4.32 Å is still within 1% lattice mismatch from β-SiC and should not reduce the propensity for β-SiC heteroepitaxy. In addition, the 5% VC should not adversely affect the thermal expansion of the substrate since the thermal expansion of pure VC lies between the thermal expansion of β-SiC and TiC as shown in Figure 28. Pure VC has a better thermal expansion match to β-SiC than pure TiC. TiC and VC are both thermodynamically stable with respect to SiC as shown in the Ellingham diagram in Figure 30. The DG°_{f} of VC and TiC are more negative than the DG°_{f} of SiC at all temperatures.

Because 5% VC alloying was not thought to significantly change the properties of TiC, DMI decided to cease using the TiC samples from Bunshah and Deshpandey and perform all subsequent experiments using the 95% TiC +5% VC crystal supplied by Walter Precht. Precht's crystal was larger, and container fewer defects than the TiC crystals supplied by Bunshah and Deshpandey. DMI believes that there is great merit to (Ti,V)C alloys as substrates for β-SiC because Mr. Precht has pointed out that (Ti,V)C alloys are much easier to zone refine than pure TiC. In January 1989, DMI submitted a SBIR Phase I proposal to the Office of Naval Technology to explore the use of (Ti,V)C monocrystalline alloys as substrates for β-SiC. The relative merits of (Ti,V)C alloys are discussed at length in this proposal.

5.5 Engineering Observations

One of the major findings of this program was the discovery that pyrolytic boron nitride (PBN) causes several practical problems when used to enclose a graphite susceptor during the CVD of SiC. The original design of the pyrolytic boron nitride successfully enhanced high temperature operation since the pyrolytic boron nitride totally enclosed the graphite susceptor. The white surface of the PBN helped to minimize emissive losses from the hot graphite susceptor. Despite the large size of the PBN susceptor arrangement, temperatures exceeding 1325°C could be easily obtained at the beginning of a run. However, the white surface of the pyrolytic boron nitride turned dark soon after the start of deposition. DMI discovered, as did J. A. Powell [22] and So et al. [14], that all β-SiC CVD growth runs are inevitably accompanied by SiC powder formation on the susceptor and along the inside walls of the silica chamber. Therefore, use of PBN was discontinued when growing from mixtures of hydrogen, methylsilane and ethylene because the temperature drop during the run was as large as 200°C due to the increased emittance of the PBN due to SiC powder deposition.

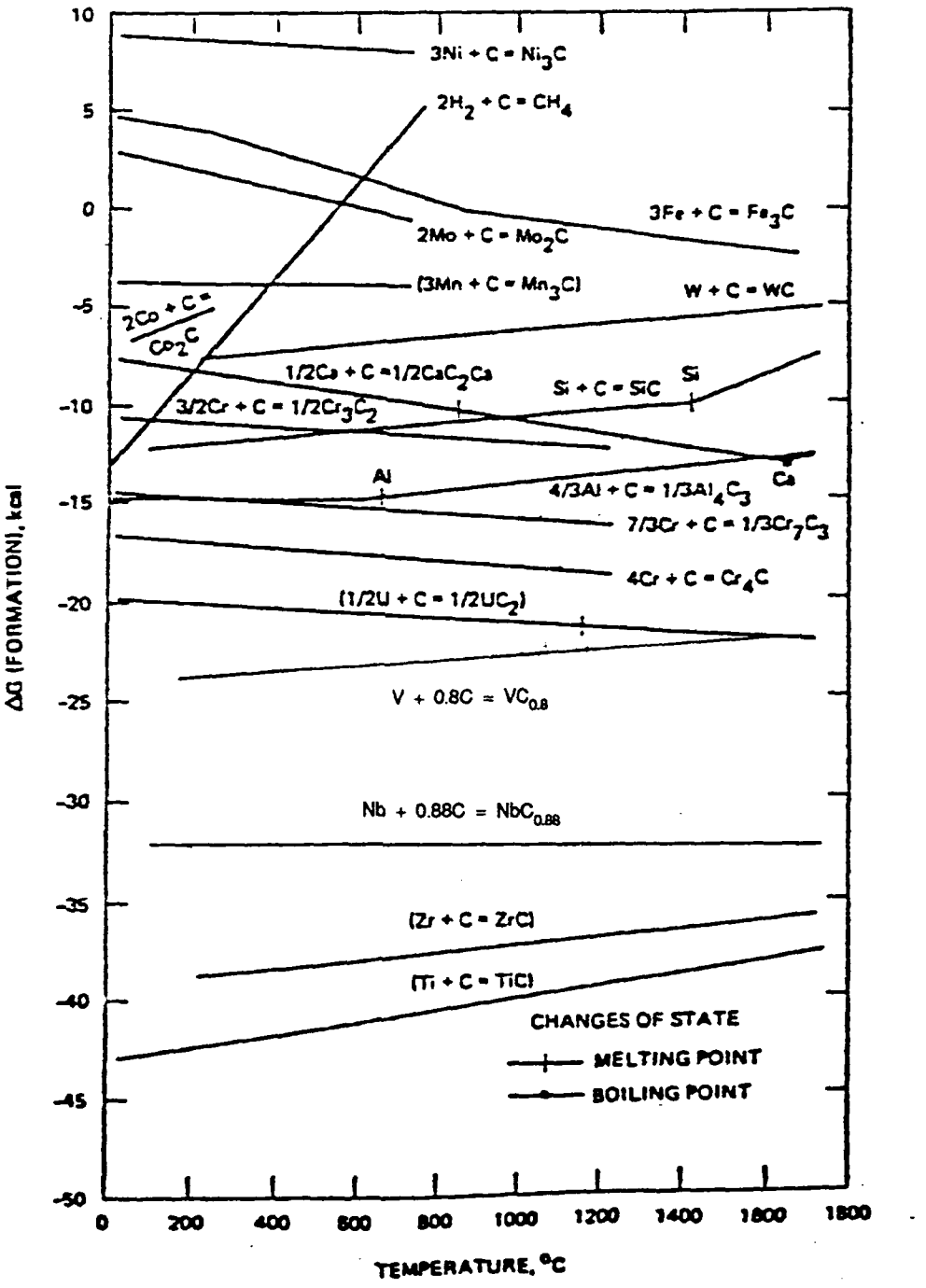

FIGURE 30. ELLINGHAM DIAGRAM FOR VARIOUS CARBIDES. The Gibbs energy of formation of TiC and VC is significantly more negative than the Gibbs energy of formation of SiC; (Ti,V)C alloys are chemically compatible with SiC. (Diagram reproduced from Reference 6, with additional data plotted from I. Barin and O. Knacke, Thermochemical Properties of Inorganic Substances, Springer-Verlag, Berlin (1973)).

PBN was found to be extremely reactive with methyl trichlorosilane producing powder thought to be a mixture of ammonium chloride and/or silicon nitride. The powder produced by the reaction between PBN and the MTS was voluminous; the powder clogged the throttle valve situated between the effluent port of the chamber and the vacuum pump. Positive identification of the powder was not made. However, the powder was thought to be ammonium chloride created by a two step reaction. At high temperature, boron nitride was thought to react with the HCl according to the reaction:

$$2BN_{(s)} + 6HCl_{(g)} = 2BCl_{3(v)} + N_{2(g)} + 3H_{2(g)} \quad (3)$$

At 1500 K, Reaction 1 has a DG°_{rxn} of 206 kJ/mol. However when boron trichloride is allowed to cool to room temperature, NH_4Cl precipitates according to the reaction:

$$BCl_{3(v)} + 1.5N_{2(g)} + 7.5H_{2(g)} = NH_4Cl_{(s)} + 0.5B_2H_{6(v)} \quad (4)$$

At room temperature, reaction 2 has DG°_{rxn} of -175 kJ/mol.

Silicon nitride may have been formed by the direct reaction of MTS with the boron nitride according to the reaction:

$$3H_{2(g)} + 3CH_3SiCl_{3(v)} + 4BN_{(s)} = 3BCl_{3(v)} + Si_3N_{4(s)} + 3CH_{4(g)} + 0.5B_2H_{6(v)} \quad (5)$$

At 1500 K, reaction 3 has DG°_{rxn} of -777 kJ/mol.

Because of the aforementioned problems, DMI decided to redesign the susceptor assembly out of graphite. Graphite has several advantages as a susceptor/pedestal for ß-SiC. Graphite is chemically compatible since an outer coating of silicon carbide is deposited on the graphite rendering it inert with respect to both methyl trichlorosilane and methylsilane. The graphite susceptor was coated with SiC by a MTS/hydrogen run prior to attempting ß-SiC heteroepitaxial growth on TiC. J. A. Powell of NASA Lewis Research Center reported that *in situ* coating of graphite susceptors produced superior results than commercially available SiC-coated graphite susceptors [23]. Powell reported that the incidence of particulate formation on the surface of his films was much less when using graphite susceptors he had coated himself.

The major problem in using an all graphite sample holder was the large emissive losses of heat since graphite has near unity emittance. The PBN pedestal with the enclosed graphite susceptor resulted in a maximum temperature of 1320°C. Direct replacement of the pyrolytic boron nitride pedestal by a graphite pedestal of identical

dimensions resulted in the attainment of a maximum temperature of only 1100°C despite the same rf power. The design was changed as discussed in Section 2 in order the minimize the total emissive area. Best results were obtained when a disk-shaped susceptor was used in contact with the TiC and radiation losses from the top were minimized by use of a PBN + graphite cap (Figure 4).

6. SUMMARY OF CONCLUSIONS

1. DMI has successfully grown heteroepitaxial β-SiC on a monocrystalline, 95% TiC + 5% VC substrate. Heteroepitaxy was achieved from 2% MTS/H_2 at 1400C, 250 torr. Correct carburization of the TiC_x surface immediately prior to β-SiC growth was critical.

2. Single phase β-SiC can be deposited from mixtures of MTS and hydrogen or mixtures of methylsilane, ethylene and hydrogen. DMI did not have time to verify whether or not heteroepitaxial β-SiC could be grown from mixtures of methylsilane and ethylene. However, it is felt that methylsilane/ethylene mixtures can be used for heteroepitaxial growth. Methyl trichlorosilane is preferred as the source gas for heteroepitaxial growth since (a) MTS does not require the use of a second hydrocarbon source to prevent co-deposition of silicon, and (b) MTS is more readily available at semiconductor-grade purities. In conclusion, MTS/hydrogen mixtures are optimal for the deposition of heteroepitaxial β-SiC.

3. Use of pyrolytic boron nitride in the susceptor substrate holder was found to be highly problematic. This is in disagreement with the use of pyrolytic boron nitride recommended by Jim Parsons [6]. Pyrolytic boron nitride was found to be unacceptable because (1) it chemically reacts with methyl trichlorosilane releasing large quantities of powder, and (2) white surface of boron nitride is inevitably coated with silicon carbide powder; the powder coating increases emittance and decreases sample temperature. Deposition of this powder results in rapid loss of temperature of the suspended platen due to increased radiation heat losses.

4. DMI found excellent agreement between the source gas mixtures found to create single phase β-SiC and thermodynamic predictions of optimal source gas compositions. In agreement with thermodynamic predictions, DMI found that the use of argon as a diluent was highly undesirable because it promoted the co-deposition of graphite or silicon.

5. In agreement with Jim Parsons, DMI found that the quality of the β-SiC film was highly dependent upon the quality of the TiC substrates. DMI observed that

subgrain boundaries in TiC caused the formation of highly distinct regions in polycrystalline β-SiC films deposited on the TiC. The best β-SiC morphology was found on a TiC/VC 95/5 alloy monocrystal provided by Walter Precht of Martin Marietta Laboratories. This crystal lacked subgrain boundaries and pinholes and was the substrate used to grow monocrystalline β-SiC. The presence of 5 mol% VC in the TiC did not prevent achievement of β-SiC heteroepitaxial growth.

6. Further research is needed in order to upgrade the reactor to improve the surface morphology of the β-SiC films. In Phase II, DMI will work with experts in CVD reactor design to improve the uniformity of the β-SiC monocrystalline films. DMI will also obtain an in-house copy of the thermochemical software SOLGASMIX-PV in order to ensure all materials used in reactor upgrades are chemically compatible with the creation of β-SiC by reaction of MTS with hydrogen.

7. DMI will submit a Phase II proposal. In Phase II, DMI will perform *in situ* doping of β-SiC films with dopants such as boron, aluminum and nitrogen. DMI also proposes to optimize growth rates, film morphology and to control the resistivity of the films. The Phase II program proposes to create useful semiconductor devices, e.g., β-SiC IMPATT diodes.

7. REFERENCES

1. J. D. Parsons, R. F. Bunshah and O. M. Stafsudd, "Unlocking the Potential of Beta Silicon Carbide," *Solid State Technology*, 133 (1985).

2. I. Mehdi, G. I. Haddad and R. K. Mains, "Microwave and Millimeter wave Power Generation in Silicon Carbide Avalanche Devices," *J. of Appl. Phys.*, 64 [3] 1533 (1988).

3. H. J. Kim and R. F. Davis, "Theoretical and Empirical Studies of Impurity Incorporation into β-SiC Thin Films during Epitaxial Growth," *J. Electrochem. Soc.* 133[11] 2350 (1986).

4. J. W. Palmour, H. S. Kong and R. F. Davis, "High-temperature Depletion-Mode Metal-oxide-semiconductor Field-Effect Transistors in Beta-SiC Thin Films," *Appl. Phys. Lett.*, 51[24] 2028 (1987).

5. H. Fuma, A. Miura, H. Tadano, S. Sugiyama, and M. Takigawa, "Fabrication of MOSFET's on the β-SiC Single Crystalline Layer Grown on Si (100) Substrate," talk delivered at ICACSC '88, Santa Clara University, December (1988).

6. J. D. Parsons, "Single Crystal Epitaxial Growth of β-SiC for Device and Integrated Circuit Applications," Novel Refractory Semiconductors, Mat. Res. Soc. Symp. Proc., 97, 271 (1987).

7. H. Matsunami, "Crystalline SiC on Si and High Temperature Operational Devices," talk delivered at ICACSC '88, Santa Clara University, December (1988).

8. A. I. Kingon, L. J. Lutz, P. Liaw and R. F. Davis, "Thermodynamic Calculations for the Chemical Vapor Deposition of Silicon Carbide," *J. Am. Ceramic Soc.*, 66 [8] 558 (1983).

9. G. S. Fischman and W. T. Petuskey, "Thermodynamic Analysis and Kinetic Implications of Chemical Vapor Deposition SiC for the Si-C-Cl-H Gas Systems," *J. Am. Ceramic Soc.*, 68 [4] 185 (1985).

10. J.D. Parsons, G. Kruaval, and J. Vigil, "β-SiC on Titanium Carbide for Solid State Devices," talk delivered at ICACSC '88, Santa Clara University, December (1988).

11. J. A. Powell, "Silicon Carbide: Progress in Crystal Growth," Novel Refractory Semiconductors, Mat. Res. Soc. Symp. Proc., 97, 159 (1987).

12. T. M. Bessmann, "SOLGASMIX PV, A Computer Program to Calculate Equilibrium Relationships in Complex Chemical Systems, ORNL-TM-5775, Oak Ridge National Laboratory, April (1977).

13. K. E. Spear, "Applications of Phase Diagrams and Thermodynamics to CVD," in Proc. of the Seventh Internation Conf. on Chemical Vapor Deposition, The Electrochem. Soc., 1 (1979).

14. M. G. So and J. S. Chun, "Growth and Structure of Chemical Vapor Deposited Silicon Carbide From Methyltrichlorosilane and Hydrogen in the Temperature Range of 1100 to 1400°C," *J. Vac. Sci. Technol.*, A6 [1] 5 (1988).

15. S. Nishino and J. Saraie, "Epitaxial Growth of Cubic SiC on Si Substrate Using Si_2H_6 - C_2H_2 - H_2 System," talk delivered at ICACSC '88, Santa Clara University, December (1988).

16. J. Chin, P.K. Gantzel and R.G. Hudson, "The Structure of Chemical Vapor Deposited Silicon Carbide," *Thin Solid Films*, 40, 57 (1977).

17. H. S. Kong, J. T. Glass and R. F. Davis, "Epitaxial Growth of β-SiC Thin Films on 6H α-SiC Substrates via CVD," *Appl. Phys. Lett.* 49 [17]1074 (1986).

18. S. Nishino and J. Saraie, "Epitaxial Growth of 3C-SiC on Si Substrate using Methyletrichlorosilane," Abstract of talk presented at 1st International Conference on Amorphous and Crystalline Silicon Carbide and Related Materials, Washington, D.C. (1987).

19. Engineering Properties of Selected Ceramic Materials, The American Ceramic Society, Columbus, OH (1966).

20. P. A. Glasow, "6H SiC Studies and Development at Seimens AG and at the Institut für Angewandte Physik at the University of Erlangen, F. R. Germany," talk delivered at ICACSC '87, Howard University, December (1987).

21. Max Yoder, private communication (1988).

22. J. A. Powell, private communication (1988).

23. J. A. Powell and L.G. Matus, "Chemical Vapor Deposition of Single Crystal β-SiC," talk delivered at ICACSC '88, Santa Clara University, December (1988).